2015

Engineering properties of saturated and biogas desaturated sand

Seth Hansen
Iowa State University

Engineering properties of saturated and biogas desaturated sand

by

Seth Hansen

A thesis submitted to the graduate faculty

in partial fulfillment of the requirements for the degree of

MASTER OF SCIENCE

Major: Civil Engineering (Geotechnical Engineering)

Program of Study Committee:
Jian Chu, Major Professor
Jeremy Ashlock
Chris Rehmann

Iowa State University

Ames, Iowa

2015

DEDICATION

This thesis is dedicated to my mother-in-law, Joni Mary Wailes, who recently lost a courageous battle with breast cancer.

January 29th, 1956 - May 28th, 2015

"She watches over the affairs of her household
and does not eat the bread of idleness. Her children arise and call her blessed;
her husband also, and he praises her:
'Many women do noble things,
but you surpass them all.'
Charm is deceptive, and beauty is fleeting;
but a woman who fears the LORD is to be praised.
Honor her for all that her hands have done,
and let her works bring her praise at the city gate."

- Proverbs 31:27-31 -

TABLE OF CONTENTS

Page

LIST OF FIGURES

Page

LIST OF TABLES

Page

ACKNOWLEDGEMENTS

First and foremost, I would like to thank my wife Heather, for her limitless and steadfast support during the preparation of this thesis. Without her, this thesis would not have been possible. When times were tough you kept encouraging me that everything would be okay and that I needed to just take one day at a time. I would also like to thank my parents, Gary and Janis, for their constant physical, emotional, and spiritual support that they have selflessly given to me from the time of my birth to this day.

I would like to thank Dr. Jian Chu for all of his advice, patience, and support throughout this project. I would also like to thank Dr. Jeramy Ashlock and Dr. Chris Rehmann for the additional support they gave me during the preparation of this thesis.

I would like to thank Bill Halterman and Bruce Erikson from the Iowa State Univeristy machine shop. These guys made the development of the plane strain apparatus possible and without their practical knowledge and foresight the fabrication process would not have gone nearly as smooth.

ABSTRACT

When a fully saturated loose sand is subjected to a seismic load the sand liquefies which results in little to no shear strength. It has been shown that by reducing the degree of saturation through the microbial denitrification process that the shear strength of sands under isotropic conditions can be greatly improved. However, previous studies have only studied the effects of biogas on isotropically consolidated samples. Soils in the ground are considered K_0 consolidated, therefore a study on the effects of K_0 consolidation of the biogas desaturated sand was performed. Triaxial undrained compression tests were performed on isotropically consolidated and K_0 consolidated loose sand specimens. The isotropically consolidated test results showed a significant increase in shear strength when Skempton's pore water pressure coefficient B-value decreased from 0.99 to 0.39. With this reduction in B-value, the loose sand went from a strain softening behavior to a strain hardening behavior by reducing the maximum excess pore pressure generated during undrained shearing. This behavior is well reported in the literature. However, the results of the K_0 consolidated triaxial samples showed much less improvement compared to the isotropically consolidated samples. It was found that by decreasing the degree of saturation the development of pore water pressure was increasingly delayed. This delay may prevent a catastrophic failure caused by brittle behavior under in-situ conditions.

It has been found that the permeability of soils can be decreased by reducing the degree of saturation. For this reason, a study on the use of the microbial denitrification method to reduce the permeability of a clean sand was performed. A series of sand column permeability tests were performed to observe the change in the coefficient of permeability with decreasing the degree of saturation using the microbial denitrification method. Using

the denitrifying bacteria, a fully saturated sand can be partially desaturated to a degree of saturation of around 70%. By reducing the degree of saturation to around 70%, the coefficient of permeability of a fully saturated sand at a void ratio of 0.65 decreased from 8.3 (10^{-4}) m/s to 2.7 (10^{-4}) under a hydraulic gradient of 0.1. Although a reduction in the permeability of 67% was found, the microbial denitrification method was found to be unsuitable for reducing the permeability of clean sands for use as an impermeable layer.

Many geotechnical structures such as slopes, embankments, and retaining walls can be approximated to plane strain conditions. To understand plane strain conditions it is better to perform actual plane strain tests rather than conventional triaxial tests. Therefore, a plane strain apparatus modeled after the Nayang Technological University plane strain device was constructed as a part of this thesis. An overview of the design and the control program has been discussed. A series of undrained and drained plane strain compression tests were performed on loose sand samples. The plane strain device was found to provide accurate and reliable results for K_0 consolidation, drained shear, and undrained shear. Therefore, this device can be used for future research projects concerned with plane strain conditions.

CHAPTER 1.

INTRODUCTION

1.1Background

In the past, most of the research into soil behavior and soil properties has been physical with little attention given to biological effects. A relatively new branch of geotechnical engineering, called Biogeotechnology, attempts to solve geotechnical engineering problems using biological methods. These methods have garnered a lot of attention in recent years as they are more environmentally friendly, more sustainable, and have lower relative costs.

One topic of interest is the capability of microbes to produce large amounts of gas. It has been well researched that a small presence of gas bubbles in sand can greatly improve the stress-strain behavior of loose sand under cyclic loading. This has been shown by a number of researchers via a number of different testing techniques including cyclic triaxial tests (Bouferra et al. 2007; Okamura and Soga 2006; Pietruszczak et al. 2003; Tamura et al. 2002; Tsukamoto et al. 2002; Xia and Hu 1991), cyclic torsional shear tests (Altun and Goktepe 2006; Sherif et al. 1977; Yoshimi et al. 1989) and shaking table tests (Eseller-Bayat 2009; He 2013; Lee and Santamarina 2007; Okamura and Teraoka 2006; Yegian et al. 2006, 2007). Grozic et al. (1999) observed that under conventional isotropically undrained triaxial compression tests, loose sand with a degree of saturation lower than about 90% exhibited strain hardening behavior. They also observed that samples with a DOS > 90% loose sand exhibited complete strain softening behavior. More recently, He et al. (2013) observed that the inclusion of tiny nitrogen gas bubbles produced by denitrifying

bacteria could cause isotropically consolidated loose sand samples to go from a completely strain softening behavior to a strain hardening behavior at a low confining stress. Therefore, microbes can be utilized to produce biogas in order to improve the strength characteristics of loose soil deposits. However, soil in-situ is not isotropically consolidated but rather K_0 consolidated. Recent studies only performed triaxial tests on isotropically consolidated specimens. Therefore, a study on the effectiveness of the biogas method under in-situ stress conditions is needed. This is one of the main objectives of this study.

The other main objective of this thesis is to construct a plane strain apparatus. Many geotechnical engineering problems such as slopes, embankments, strip footings, and retaining walls can be approximated to plane strain conditions. Data from plane strain tests are more representative of the above-mentioned applications as opposed to data collected from typical triaxial testing. Similarly, strain localization problems in the field can be better understood by performing plane strain tests (Wanatowski 2005). For these reasons, a plane strain testing apparatus was constructed as a part of this thesis for use in future research projects.

1.2Research Objectives

The objectives of this study include:

1) To study the stress-strain behavior of saturated and biogas desaturated sand with samples consolidated along the K_0 line.
2) To compare the stress-strain behavior and liquefaction resistance of biogas desaturated sand under both isotropic consolidation and K_0-consolidation conditions.

3) To measure the hydraulic conductivity of biogas desaturated sand at varying degrees of saturation.
4) To construct a plane strain testing device to be used for future research
5) To perform undrained and drained plane strain tests on loose sand

1.3Project Scope

The scope of this study includes:

1) To perform isotropic consolidated and K_0 consolidated undrained triaxial compression tests on loose sands with varying degrees of saturation
2) Compare and contrast the isotropic and K_0 consolidated triaxial test results
3) Perform hydraulic conductivity tests on samples with varying degrees of saturation
4) Fabricate a plane strain apparatus and perform undrained and drained plane strain compression tests on loose sand.

1.4Outline of Thesis

This thesis is composed of seven chapters. Chapter 2 includes a literature review on critical state, behavior of sandy soil under undrained conditions, current methods of desaturation, microbial methods in geotechnical engineering, and plane strain testing. Chapter 3 discusses the materials used in this study. Chapter 4 discusses the triaxial testing equipment, testing procedures, and the results of the triaxial tests. Chapter 5 presents the results of the permeability tests performed on saturated and biogas desaturated sand. Chapter 6 discusses the fabrication and design of the plane strain apparatus constructed in

this study as well as the results of the plane strain tests. Chapter 7 includes the conclusions obtained as a result of this research and recommendations for further studies.

CHAPTER 2.

LITERATURE REVIEW

2.1Introduction

The following sections comprise the literature review. Topics to be discussed include: critical state, behavior of sandy soil subjected to undrained conditions, methods of desaturation, microbial methods in geotechnical engineering, and plane strain testing.

2.2Critical State of Sands

The void ratio of soil plays a significant role in the behavior of the soil during shearing. Dense materials will tend to dilate while loose materials tend to contract. Therefore, it is natural to assume that there exists a void ratio at which the material neither dilates nor contracts. In the early 1930's, Arthur Casagrande proposed the concept of critical state in order to relate volume change, sample density, and confining pressure during shearing (Casagrande 1936). Casagrande found that there is a critical void ratio that depended only on the confining pressure during shearing. Schofield and Wroth (1968), further built on the idea of the critical void ratio introducing critical state soil mechanics which characterized soil behavior in an elasto-plastic framework. According to Schofield and Wroth (1968) the critical state can be defined as a state of continued plastic shearing without any change in volume or effective stresses.

According to critical state soil mechanics, there is a unique relationship between the void ratio and the effective stresses acting on a soil. Therefore, the critical state line (CSL) can be used to describe the critical state in both the *e-p'* and *q-p'* planes. Figure 2-1

depicts the concept of the critical state line for both normally consolidated undrained (CU) test and a normally consolidated drained (CD) test. During the CU test, the void ratio is held constant so the mean effective stress (*p'*) decreases in the *e-p'* plane until reaching the CSL. In the CD test, volume is allowed to change so the void ratio decreases while *p'* increases until the CSL is reached.

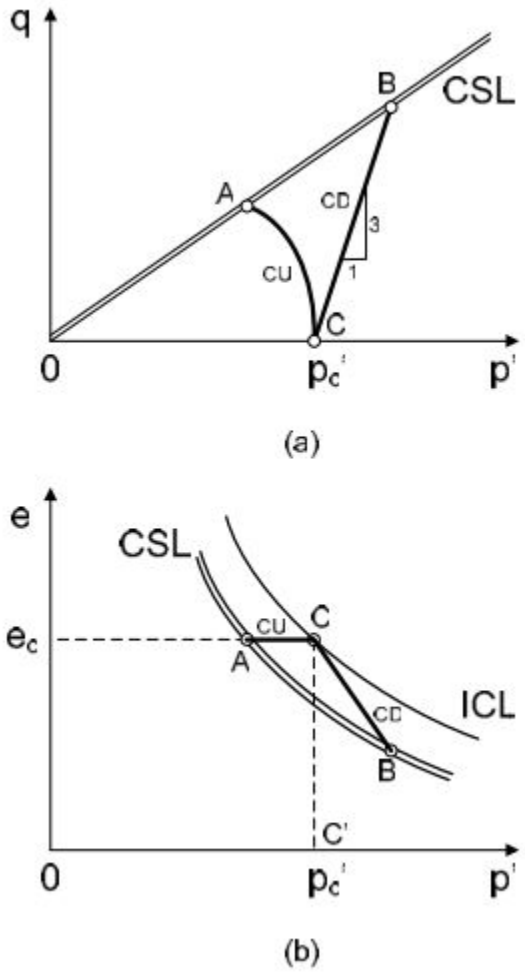

Figure 2-1.Representation of critical state line on (a) q-p' plot and (b) e-p' plot (Wanatowski 2005)

Another concept similar to the critical state is that of steady state. The concept of steady state was first proposed by Poulos (1981) as a state of continuous deformation at constant

volume, normal effective stress, shear stress, and constant velocity. The steady state line (SSL) is obtained from performing undrained tests while the CSL is obtained from drained tests. Although the definitions of the SSL and CSL are not the same, for practical purposes they can be assumed equal (He 2013).

2.3Behavior of Sandy Soil Under Undrained Conditions

2.3.1Response of Sand in Undrained Triaxial Compression

As mentioned above, the response of sand in undrained triaxial compression can vary depending on whether the sample is above, at, or below the critical void ratio. Figure 2-2 shows five different undrained responses of sand in triaxial compression. In the figures (a) through (c) the samples exhibit dilative behavior while in figures (d) and (e) the samples exhibit contractive behavior. In pattern (a) the sample exhibits increasing mean effective stress all the way up to the CSL. Pattern (b) shows a decreasing mean effective stress *p'* until reaching the CSL at which point the mean effective stress and deviator stress increase along the CSL. Pattern (c) exhibits a decreasing mean effective stress until reaching the CSL. Once reaching the CSL, the mean effective stress increases along the CSL. Pattern (c) also exhibits an early peak in the deviator stress followed by a decrease in the deviator stress until reaching the CSL. Once the sample reaches the CSL, the deviator stress increases and strain hardening occurs. The point where pattern (c) reaches the CSL is called the quasi-steady state (Alarcon-Guzman et al. 1988). The results of pattern (d) show contractive behavior all the way until the sample reaches the CSL. Pattern (e) exhibits contractive behavior until the deviator stress reaches zero. At this point, the sample has

undergone complete liquefaction which can be seen in the deviator stress vs. strain figure for pattern (e). The deviator stress reaches zero at complete liquefaction.

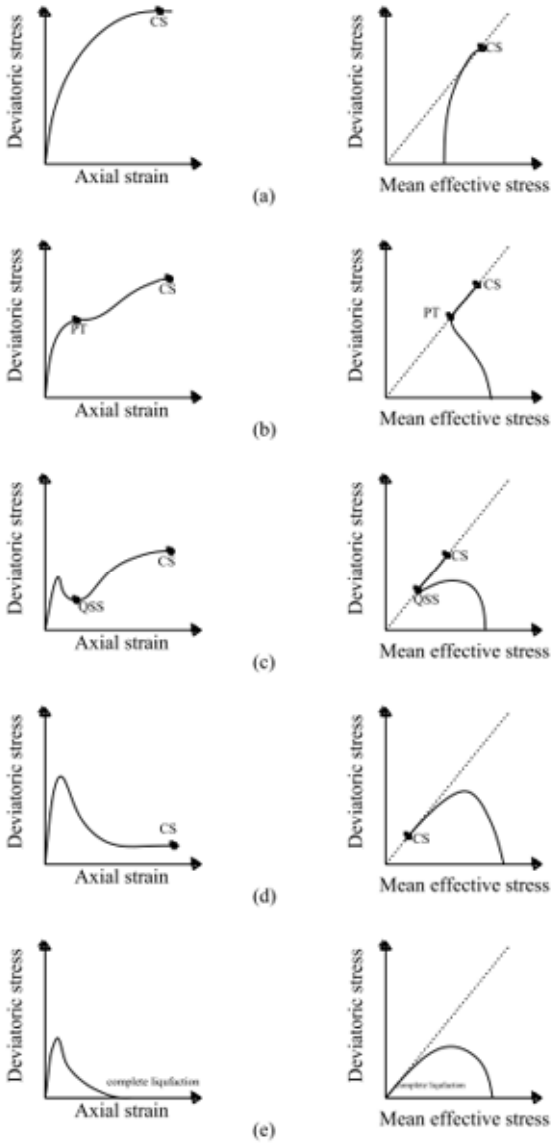

Figure 2-2. Undrained responses under triaxial compression (He 2013)

Whether or not sand will exhibit contractive or dilative behavior can be explained by its relative position with respect to the CSL on the *e-p'* plane. If the initial void ratio is above the CSL, then the soil will exhibit contractive behavior. If the initial void ratio is

below the CSL, then the sample will exhibit dilative behavior. To determine whether a sample will contract or dilate, Been and Jefferies (1985) introduced the concept of the state parameter. The state parameter ψ, can be used to relate the initial void ratio to that of the CSL as follows:

$$\psi = e - e_{cr} \tag{1}$$

where e is the initial void ratio, e_{cr} is the critical void ratio at the same mean effective stress. A point above the CSL will have a positive value of the state parameter and will exhibit contractive behavior while a point below the CSL will have a negative state parameter and will exhibit dilative behavior. Figure 2-3 is a representation of the state parameter and how it relates to the CSL and critical state.

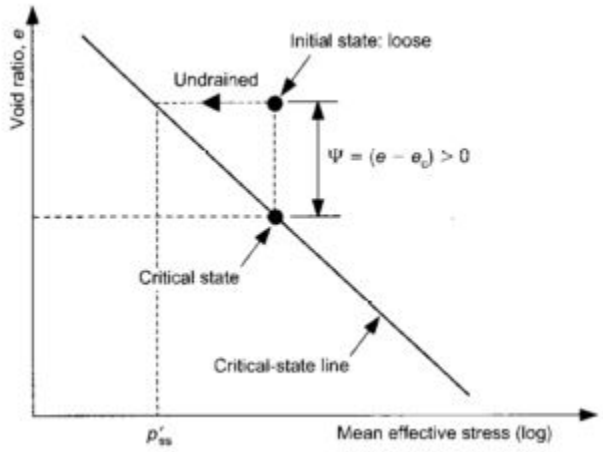

Figure 2-3. Schematic displaying the concept of the state parameter (Yang 2002)

2.3.2Effects of Gas on the Stress-Strain Behavior of Sand

It has been well researched that a small presence of gas bubbles in sand can greatly improve the stress-strain behavior of loose sand under cyclic loading. This has been shown by a number of researchers via a number of different testing techniques including cyclic

triaxial tests (Bouferra et al. 2007; Okamura and Soga 2006; Pietruszczak et al. 2003; Tamura et al. 2002; Tsukamoto et al. 2002; Xia and Hu 1991), cyclic torsional shear tests (Altun and Goktepe 2006; Sherif et al. 1977; Yoshimi et al. 1989) and shaking table tests (Eseller-Bayat 2009; He 2013; Lee and Santamarina 2007; Okamura and Teraoka 2006; Yegian et al. 2006, 2007). Under monotonic loading, the behavior has been shown to depend on the density of the sand and stability of the gas. Grozic et al. (1999) observed that under conventional isotropically undrained triaxial compression tests, loose sand with a degree of saturation lower than about 90% exhibited strain hardening behavior. They also observed that loose samples with a DOS > 90% exhibited complete strain softening behavior. Rad et al. (1994) studied the presence of gas on dense sand under monotonic loading and found that the presence of gas may be detrimental to the undrained strength of dense sand. It was found that as the gas content (dissolved or in free form) increased, the weaker the specimen behaved under undrained loading conditions. Rad et al (1994) also found that the solubility of gas played a significant role in the behavior under undrained conditions. The higher the solubility of the gas, the greater the amount of gas released and the weaker the specimen became during undrained shearing.

He et al. (2013) observed that the inclusion of tiny nitrogen gas bubbles produced by bacteria could cause isotropically consolidated loose sand samples to go from a completely strain softening behavior to a strain hardening behavior at a low confining stress (see Figure 2-4). Most studies relating to the presence of gas in triaxial testing were performed on isotropically consolidated sand samples. However, soils in-situ are K_0 consolidated therefore, a study on the effects of consolidation on the biogas desaturation method has yet to be performed.

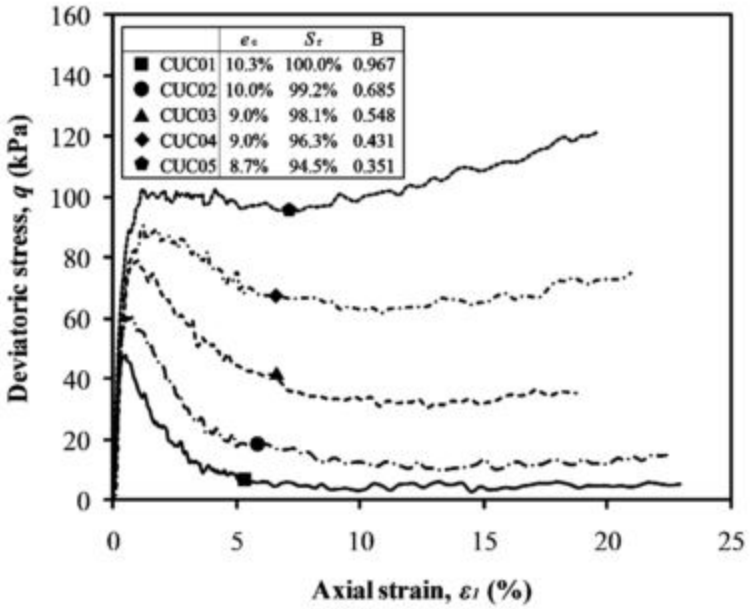

Figure 2-4. Undrained response of isotropically consolidated microbially desaturated sand (He and Chu 2013)

2.4Methods of Desaturation

The following sections outline several methods used as a means of desaturation. These include air injection, water electrolysis, sodium perborate, microbial denitrification, and the sand compaction pile method. Of these methods, the chemical and biological methods are preferred due to the production of a more uniform distribution of gas bubbles. To be a practical means of improvement, the method must also provide a good estimation of the degree of saturation after treatment. A brief summary of these methods is given below.

2.4.1Air Injection Method

Okamura et al. (2011) researched a method of injecting air as a means of desaturation into a liquefiable soil. Air was injected via a plastic pipe at the bottom of a

saturated sand layer at a depth of 6 m. At the injection point, small holes were drilled in the pipe and pressurized air was supplied via flexible tubing down to the injection point. Electrical resistivity and 3-D tomography were used to observe the reduction in degree of saturation. The results showed that the method was effective up to 4 m around the injection point. To investigate the reduction of saturation, the samples were frozen and analyzed in the lab. The degree of saturation ranged from 88% to 98%. After thawing, the samples were then tested under cyclic loading in a triaxial cell to determine the actual increase in liquefaction resistance. The tests showed that the desaturated samples had an increase in liquefaction resistance by a factor of 2 relative to the fully saturated tests.

2.4.2Water Electrolysis Method

The water electrolysis method was used by Yegian et al. (2007) to desaturate a loose sand in a laminar box. The sand used was prepared by the water sedimentation method and had a relative density of around 20%. Through the process of electrolysis, hydrogen and oxygen gas were produced at the cathode and anode respectively. The cathode was placed at the bottom of the box and the anode at the top. A current of 525 mA was applied for 1.5 and 3 hours in two different tests. This method reduced the degree of saturation from a fully saturated state to a degree of saturation of 96.3%. The fully saturated and partially saturated sand was subject to cyclic loading at a frequency of 4 Hz. The pore pressure ratios reached unity in only 2 cycles of loading for the fully saturated state while the partially saturated sample showed significant reduction in the maximum pore pressure ratio indicating liquefaction did not occur in the loose sand. The amount of gas was estimated through the use of Faraday's law:

$$n = \left(\frac{I}{4F} + \frac{I}{2F}\right)\Delta t \quad (2)$$

where n is the amount of hydrogen and oxygen gas in moles, I is the applied current, Δt is the time that the current is applied, and F is Faraday's constant (96,485 C/mol). Once the amount of gas generated was determined, it can be converted into volume via the ideal gas law:

$$PV=nRT \quad (3)$$

Where P is the absolute pressure (Pa), T is the absolute temperature (K), V is the volume, n is the number of moles which was calculated in equation (2), and R is the ideal gas constant (8.214 Pa m^3/mol). However, this process is not 100% efficient so the actual amount of gas is less than that estimated by equation (3).

2.4.3Sodium Perborate

Application of chemicals is another means of desaturation. Eseller-Bayat (2009) studied the use of sodium perborate to increase the liquefaction resistance through desaturation. In this method, sodium perborate is hydrolyzed which produces hydrogen peroxide. The hydrogen peroxide then decomposes into water and oxygen gas. These two processes are highlighted by equations (4) and (5) respectively.

$$2(NaBO_3 \cdot H_2O) + 2H_2O \rightarrow 2H_2O_2 + 2BO_3^{3-} + 2Na^+ + 4H^+ \quad (4)$$

$$2H_2O_2 \rightarrow 2H_2O + O_2 \uparrow \quad (5)$$

Eseller-Bayat (2009) also showed that the gas was very stable even at high hydraulic gradients for both vertical and horizontal flow.

2.4.4Microbial Denitrification

Desaturation can also be obtained through the use of microbial processes. Common types of gases produced by microbial processes include: CO_2, H_2, CH_4, and N_2. Microbial processes that produce insoluble and chemically-inert gases are ideal and will be able to retain in soil for a longer period of time. Of the before mentioned gases, N_2 exhibits both characteristics of low solubility and inertness. N_2 can be produced in large quantities through the process of denitrification. Microbial denitrification is the process of nitrates being reduced stepwise to nitrogen gas. This makes microbial denitrification an ideal candidate for desaturation (He 2013; Rebata-Landa and Santamarina 2012). The amount of nitrogen gas produced can be controlled by limiting the nutrients and can be estimated with a fair degree of accuracy. This topic will be discussed in greater depth later on in this thesis

2.4.5Sand Compaction Piles

Sand compaction piles (SCP) have been used since the 1970's to improve the liquefaction resistance of loose sand deposits. SCP's effectiveness is attributed to the densification of the foundation soils and the increase in lateral stresses. However, Okamura et al. (2003) observed that the degree of saturation in sands improved by the SCP method had a degree of saturation of 77% for the sand piles and 91% for the improved sand layers. It was concluded that the reduction in degree of saturation further increased the resistance to liquefaction.

2.5Microbial Methods in Geotechnical Engineering

In the past, most of the research into soil behavior and soil properties has been physical with little attention given to biological effects. A relatively new branch of geotechnical engineering, called Biogeotechnology attempts to solve geotechnical engineering problems using biological methods. These methods have garnered a lot of attention in recent years as they are more environmentally friendly, more sustainable, and have lower relative costs. The following is a review of these biological methods.

2.5.1Biocementation & Bioclogging

The process of binding soil particles together through the use of microbes and certain types of additives is called biocementation. Biocement can be used to improve the shear strength of soil (biocement) or to reduce the permeability of soil (bioclogging). In biocement, particles are cemented together by the precipitation of minerals in the pore spaces between soil particles. In bioclogging, material is precipitated between the individual soil grains thereby reducing the porosity.

2.5.1.1Urease Producing Bacteria

The most commonly researched biocement is microbial induced carbonate precipitation (MICP). MICP utilizes the urea hydrolyzing process to raise the pH of the environment, which causes the precipitation of calcium carbonate or calcite in a calcium rich environment. This process occurs in two steps. The first step is the hydrolysis of urea by urease enzymes that are produced by bacteria.

$$NH_2 - CO - NH_2 + 3H_2O \rightarrow 2NH_4^+ + 2OH^- + CO_2 \quad (6)$$

Hydroxide is produced from the formation of ammonia which causes a rise in the pH. This rise in pH causes the precipitation of calcite in a calcium rich environment.

$$Ca^{2+} + CO_3^{2-} \rightarrow CaCO_3 \downarrow \quad (7)$$

Numerous studies have been done in recent years to study the physical behavior, optimization, and potential applications of MICP to geotechnical engineering. The following is a review of recent research performed on the MICP process. DeJong et al. (2010) summarized that strength, stiffness, compressibility, and permeability could all be significantly improved through biological methods. To monitor the cementation process over time, wave propagation methods were proven effective by measuring the soil stiffness through the use of shear waves (DeJong et al. 2006, 2010; van Paassen et al. 2010). Multi-step injection methods were proposed to better promote bacteria fixation and distribution in sands (Harkes et al. 2010; Whiffin et al. 2007). Utilizing this multi-step method van Paassen et al. (2010) performed tests with 100 m^3 of granular soil in a concrete chamber and observed that it is feasible to utilize MICP at a larger scale. Achal et al. (2013) concluded that MICP also has the potential for self-healing concrete structures by showing increased strength and durability of cracked mortar cubes treated with MICP.

The MICP process can also be used to reduce the permeability of soil to control seepage (Chu et al. 2012b; Stabnikov et al. 2011). It was found that a small layer (≈ 1mm) of MICP could effectively reduce the permeability of the soil by 3 orders of magnitude. This reduction could potentially enable construction of aquaculture ponds or reservoirs in sand (Stabnikov et al. 2011).

2.5.1.2Iron-reducing bacteria

Another source of biocement includes iron-reducing bacteria. Iron-reducing bacteria reduce iron from ferric to ferrous. The ferrous iron can then form a precipitate of ferrous hydroxide which fills the space between the pores and binds soil particles together.

Chu et al. (2011) concluded that iron-reducing biocement worked better as a bioclogging agent rather than for cementation. Iron-reducing bacteria was found to reduce the permeability of sand by four orders of magnitude (Chu et al. 2011).

2.5.2Biogenic gas generation

Microbial metabolic processes produce various types of biogenic gases. The most common types of biogenic gases produced through microbial metabolic processes are CO_2, H_2, CH_4, and N_2. The properties of these gases are given below in Table 2-1. As mentioned earlier, N_2 shows the most promise for soil improvement due to its low solubility and low reactivity. Carbon dioxide has a high solubility in water, methane and hydrogen are both combustible, and methane is considered a greenhouse gas. Therefore, nitrogen gas generation was chosen for use in this study.

Table 2-1. Common types of biogenic gases and properties

Type of Biogenic Gas	Henry's constant *kh* (M/atm) (Wilhelm et al. 1977)	Properties
Carbon Dioxide CO_2	3.4×10^{-2}	High solubility
Hydrogen H_2	7.8×10^{-4}	Combustible
Methane CH_4	1.4×10^{-3}	Combustible & Greenhouse Gas
Nitrogen N_2	6.5×10^{-4}	Low solubility & Inert

2.5.3Microbial Denitrification

Microbial denitrification is the process of nitrates being reduced stepwise to nitrogen gas. In previous studies (He and Chu 2013; He et al. 2014), Potassium Nitrate (KNO_3) was used as the nitrogen source and ethanol (C_2H_5OH) was used as the electron donor as shown in equation. This study utilized glucose ($C_6H_{12}O_6$) as the electron donor rather than ethanol as it is more environmentally friendly than ethanol. The amount of

nitrogen produced is the same in both reactions and depends on the initial concentration of nitrate. The reaction for ethanol and glucose is shown in equation 8 and 9 respectively.

$$5C_2H_5OH + 12KNO_3 \rightarrow 10CO_2 + 6N_2 + 9H_2O + 12KOH \quad (8)$$

$$5C_6H_{12}O_6 + 24KNO_3 \rightarrow 30CO_2 + 12N_2 + 18H_2O + 24KOH \quad (9)$$

Many other factors also influence the denitrification of nitrate. Presence of oxygen, organic carbon, nitrogen oxides, inhibitors, as well as environmental factors such as pH and temperature all play a significant role in the efficiency of the denitrification process (Knowles 1982).

Oxygen affects both the formation and activity of the denitrifying enzymes. John (1977) monitored the effect of oxygen on cultures of *Paracoccus denitrificans* and *Escherichia coli* and observed that when oxygen is depleted the denitrification process begins, but once oxygen was reintroduced into the environment the denitrification process stopped immediately. Saleh-Lakha et al. (2009) also found that presence of oxygen gas causes more nitrous oxide to be formed than nitrogen. The presence and availability of electrons from organic carbon sources is also an important factor in the denitrification process (Knowles 1982). Stanford et al. (1975) showed that denitrifying activity was closely related to the extractable reducing sugars. Environmental factors such as pH and temperature also affect the reduction of nitrate. The denitrification rate is positively related to the pH with the ideal pH between 7 and 8 (Knowles 1982). Saleh-Lakha et al (2009) showed that low pH decreased the denitrification efficiency and that intensive activity occurred in the range of pH 6 to 8. It has also been reported by several researchers (Blaszczyk et al. 1985; Glass and Silverstein 1998; van Passen et al. 2010) that at high

concentrations of nitrate, nitrite will accumulate and prevent any further nitrate reduction. Blaszczyk et al. (1985) observed that with nitrate concentrations above 3g/L around 1 g/L of nitrite was formed.

2.6Plane Strain Testing

2.6.1Plane Strain in Geotechnical Engineering

Plane strain conditions occur when one dimension (e.g. y-direction) of the structure is very large with respect to the other two dimensions (x and z directions). In this scenario, the strain normal to the x-z plane (ε_y) and the shear strains (γ_{xy},γ_{yz}) are assumed to be zero. Many geotechnical engineering problems such as slopes, embankments, and retaining walls, can be approximated to plane strain conditions (see Figure 2-5). Data from plane strain tests are more representative of the above-mentioned applications as opposed to data collected from typical triaxial testing. Similarly, strain localization problems in the field can be better understood by performing plane strain tests (Wanatowski 2005).

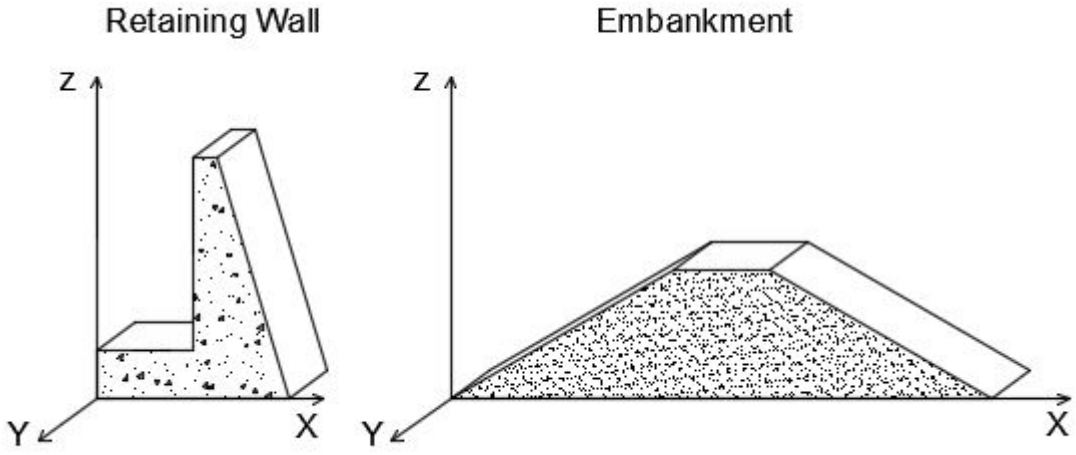

Figure 2-5.Examples of plane strain problems in geotechnical engineering

The importance of using parameters found under plane strain conditions has been shown by a number of researchers. The importance of using strength characteristics found under plane strain conditions for stability analysis was highlighted in the mid to late 1950's (Bishop 1955; Little and Price 1958). Also, the importance of shear strength and strain localization under plane strain conditions has been investigated by a number of researchers (Alshibli et al. 2004; Bishop 1966; Cornforth 1961; Green 1971; Lee 1970; Marachi et al. 1981; Wanatowski 2005). Ko and Davidson (1973) found that shear strength parameters found from axisymmetric triaxial tests resulted in conservative foundation designs. However, due to the high susceptibility of sample imperfections of plane strain tests, the onset of sudden failure can occur much sooner in plane strain tests than in triaxial tests (Lee 1970; Marachi et al. 1981).

Early on in plane strain testing, it was shown that the shear strength of granular materials under plane strain conditions was higher than under axisymmetric conditions (see Figure 2-6). It was shown that the difference between plane strain test results and triaxial test results became higher with increasing soil density (Cornforth 1964; Green and Reades 1975; Green 1971; Oda et al. 1978; Rowe 1969). A number of researchers (Barden et al. 1969; Bishop 1966; Cornforth 1964; Green and Reades 1975; Lee 1970; Marachi et al. 1981) also showed that plane strain samples were stiffer and had less volume change compared to triaxial test samples.

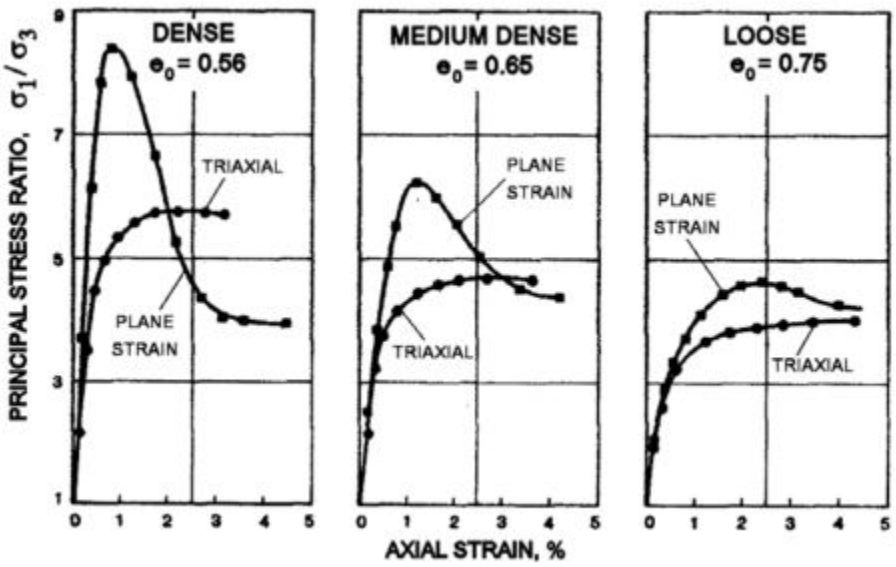

Figure 2-6.Stress-strain relationship between plane strain and triaxial test results (Marachi et al. 1981)

2.6.2Previous Plane Strain Devices

Plane strain problems such as slopes, embankments, and retaining walls are typically associated with shear bands. Shear bands in soil elements are the localization of deformation in a relatively thin zone of intense shearing (Vermeer 1990). Figure 2-7 shows a schematic of a shear band. Due to this, a large number of research projects have been devoted to the formation and characteristics of shear bands.

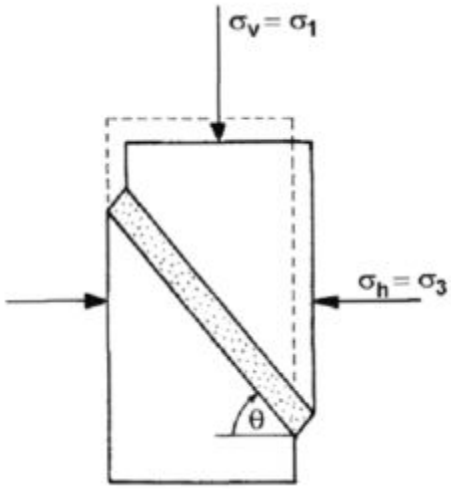

Figure 2-7.Example of shear band in soil sample (Vermeer 1990)

Over the years, several different types of plane strain and biaxial devices have been developed by a number of different research groups in order to study the characteristics of soils under plane strain conditions (Alshibli et al. 2004; Arthur et al. 1985; Bishop 1958; Campanella and Vaid 1973; Cornforth 1961, 1964; Drescher et al. 1990; Duncan and Seed 1966; Finno et al. 1996, 1997; Hambly and Roscoe 1969; Hambly 1969, 1972; Lee 1970; Leussink and Wittke 1964; Tatsuoka et al. 1986, 1994; Topolnicki et al. 1990; Yasin et al. 1999). While not an exhaustive list, a good summary of these devices is given in Table 2-2.

Table 2-2. Summary of previous plane strain devices

Location	Specimen Size (W x L x H) mm	σ_2 measurement	Remarks	Reference
Imperial College, London UK	51 x 406 x 102	Yes	Null Technique used to measure σ_2	Bishop (1958), Cornforth (1961,1964)
Technical University of Karlsruhe, Germany	200 x 1000 x 600	Yes	Large scale testing	Leussink & Wittke (1964)
University of California, Berkley, USA	28 x 71 x 61 28 x 71 x 71	No	Side plates made from Stainless Steel	Duncan & Seed (1966) Lee (1970)
University of Cambridge, UK	70-130 x 70-130 x 50	Yes	σ_1, σ_3: Aluminum plates σ_2: Glass plates	Hambly & Roscoe (1969) Hambly (1969,1972)
University of British Columbia, Canada	25 x 100 x 57	Yes	Both side plates made of stainless steel	Campanella & Vaid (1973)
University College, London, UK	100 x 100 x 100	Yes		Arthur et al. (1985) Yasin et al. (1999)
University of Karlsruhe, Germany	45-133 x 45-133 x 50	Yes	Modification of Hambly (1969) device	Topolnicki et al. (1990)
University of Minnesota, USA	40 x 80 x 140	No	Unrestrained bottom	Drescher et al. (1990)
Northwestern University, USA	40 x 80 x 140	Yes	Modification of Drescher et al. (1990) device	Finno et al. (1996,1997)
Laboratoire 3S-IMG, Grenoble, France	35 x 90-135 x 75-350	No	Unrestrained top	Desrues et al. (1985,1996) Desrues & Viggiani (2004)
University of Tokyo, Japan	40 x 80 x 105 80 x 160 x 140	Yes	ε_1 measured by proximity sensors	Tatsouka et al. (1986,1994) Yasin et al. (1999)
Louisiana State University, USA	60 x 120 x 180	No	Unrestrained bottom	Alshibili et al. (2004)
Nanyang Technological University, Singapore	60 x 60 x 120	Yes	Measured σ_2 to observe formation of shear band	Wanatowski (2005)

The earliest plane strain device found in the literature was designed at Imperial College in London in the early 1960's (Cornforth 1961, 1964). In this design, silicone grease was used in-between the rigid plates and the sample membrane. The intermediate stress was measured using the null technique. Cornforth (1961, 1964) observed that the shear band formed as the sample reached the ultimate state. Figure 2-8 depicts a plane strain sample at the end of the test using the Imperial College plane strain device.

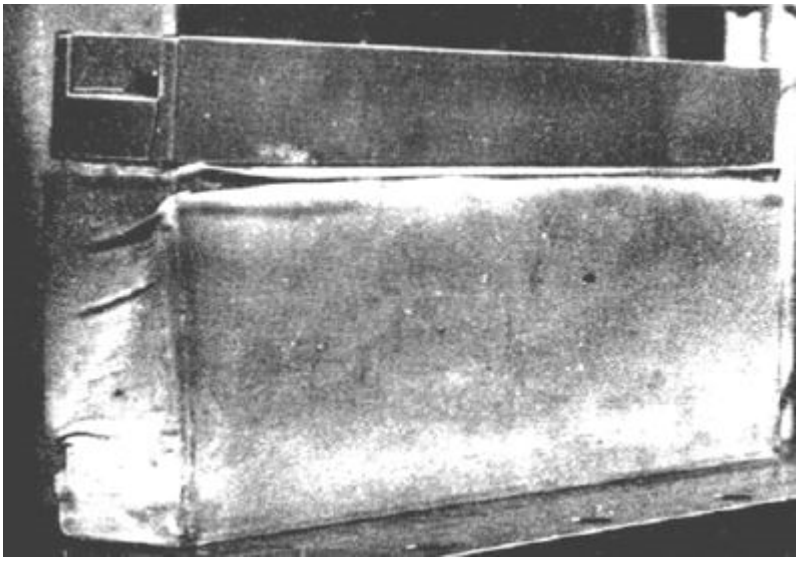

Figure 2-8.Plane strain specimen from Imperial College plane strain apparatus at the end of a test (Cornforth 1961)

Drescher et al. (1990) developed a biaxial testing device in order to study the growth of shear bands. The base pedestal was attached to a linear bearing platform (see Figure 2-9). This unique feature allowed for lateral displacements during the formation of the shear band. This effectively reduced the effects of the rigid boundaries. The plane strain condition was imposed by two rigid walls. This biaxial device did not measure the out-of-plane stress (σ_2). A schematic of the device is given in Figure 2-10.

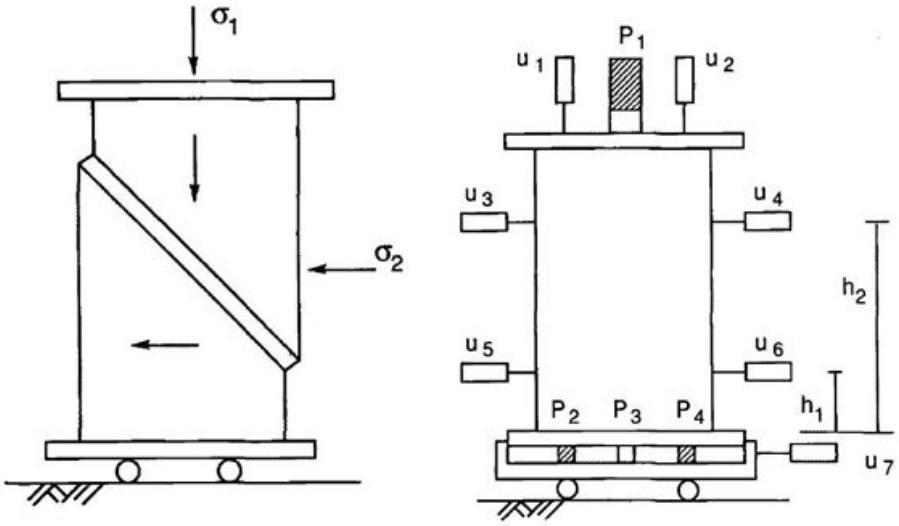

Figure 2-9.Schematic of biaxial device (Drescher et al., 1990)

Using this device, Drescher et al. (1990) observed that the shear band formed prior to the peak deviator stress. Using X-ray techniques, Han and Vardoulakis (1991) observed that shear bands formed in dense samples but not in loose samples. They also concluded under undrained conditions, the shear band formed during the strain softening portion of the test; under drained, conditions the shear band formed during the strain hardening portion of the test.

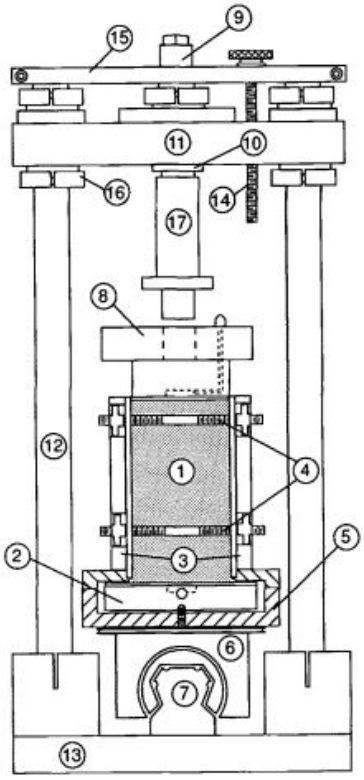

Figure 2-10. Design of biaxial device (Drescher et al., 1990)

Harris et al. (1995) further modified the biaxial device originally designed by Drescher et al. (1990). The modification included adding 4 internal load cells into the aluminum side plate in order to measure the out-of-plane stresses during shear. The other side plate was a Plexiglass® window to observe the formation of the shear band. Using this modified device, Harris et al. (1995) and Finno et al. (1996, 1997) observed that shear bands can develop in loose specimens. However, they observed that the strain localization patterns can be quite different even for similar specimens. Finno et al. (1996, 1997) observed that the shear band occurred prior to the maximum effective stress ratio.

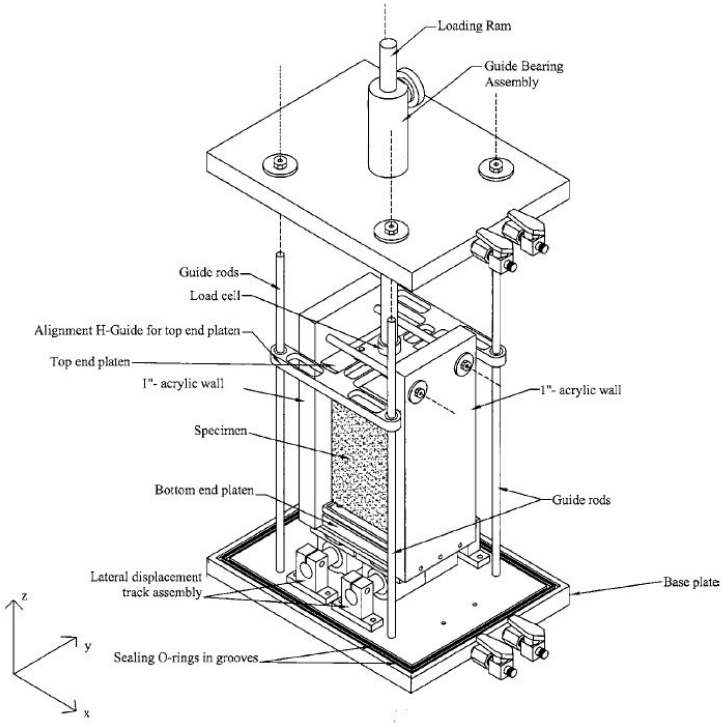

Figure 2-11. Louisiana plane strain apparatus (Alshibli et al., 2004)

Alshibil et al. (2004) described the Louisiana Plane Strain Device (LA-PSA) shown in Figure 2-11. The main feature of the LA-PSA is the flexibility in applying the bottom boundary condition. The bottom boundary could either be fixed or allowed to displace laterally along a lateral displacement assembly. The plane strain condition was imposed by two acrylic walls. The acrylic walls had the added benefit of being transparent so that the shear band could be visually observed during the test. The LA-PSA allowed for samples of various sizes up to 60 mm wide x 120 mm long x 180 mm high. Alshibil et al. (2004) used this device to observe the differences between the unrestrained and restrained boundary condition. They observed that a sample tested with a fixed boundary showed a higher friction angle than that of a sample test with a non-restrained bottom platen (see Figure 2-12).

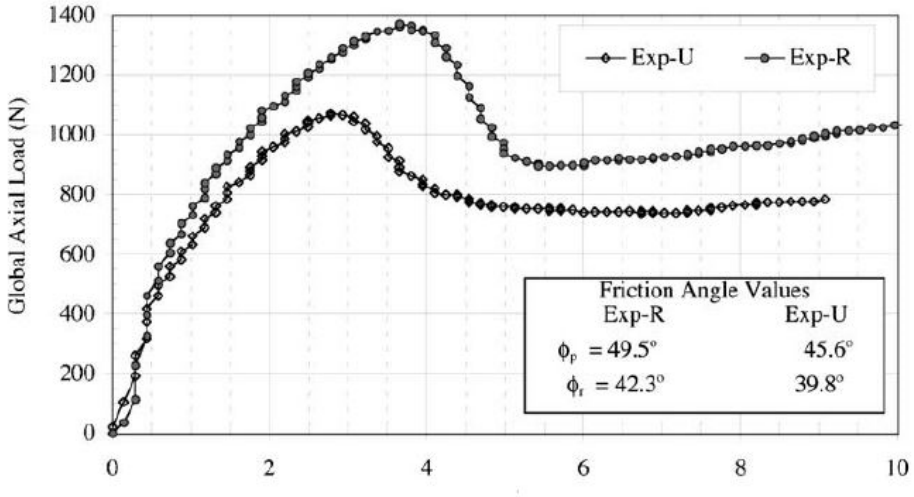

Figure 2-12. Comparison between restrained and unrestrained boundary condition (Alshibli et al., 2004)

The device chosen to construct in this study was modeled after the plane strain apparatus described by Wanatowski (2005). A photograph and a schematic drawing of this device is given in Figure 2-13 and Figure 2-14 respectively. This plane strain device was developed by modifying an existing triaxial cell. This plane strain device allowed for the measurement of the out-of-plane stress through the use of 4 pressure cells embedded in the rigid side plates and utilized the free end technique described by Rowe and Barden (1964) to reduce the boundary effects. The device featured a prismatic soil specimen (60 x 60 x 120 mm). This particular device has been used for a number of different research projects including: instability of sands under plane strain conditions (Chu and Wanatowski 2008, 2009; Chu et al. 2012a; Wanatowski et al. 2010) effect of specimen preparation on stress-strain behavior in plane strain tests (Wanatowski and Chu 2008), static liquefaction of sand in plane strain (Wanatowski and Chu 2007a), and the effect of loading mode on strain softening behavior under plane strain (Chu and Wanatowski 2009).

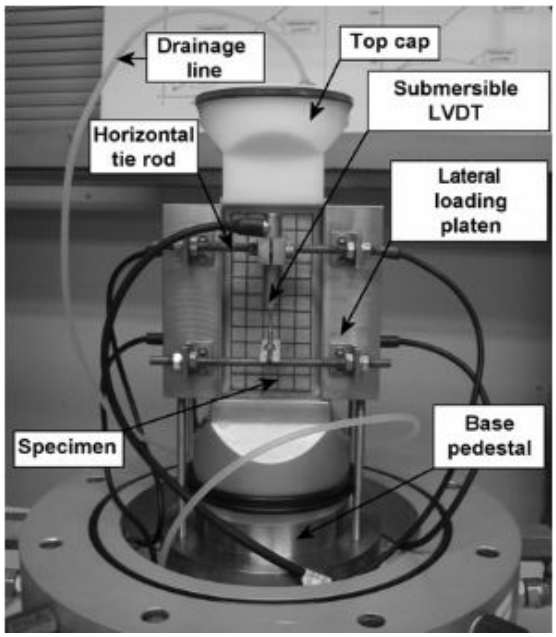

Figure 2-13. Photograph of the plane strain developed at NTU (Wanatowski 2005)

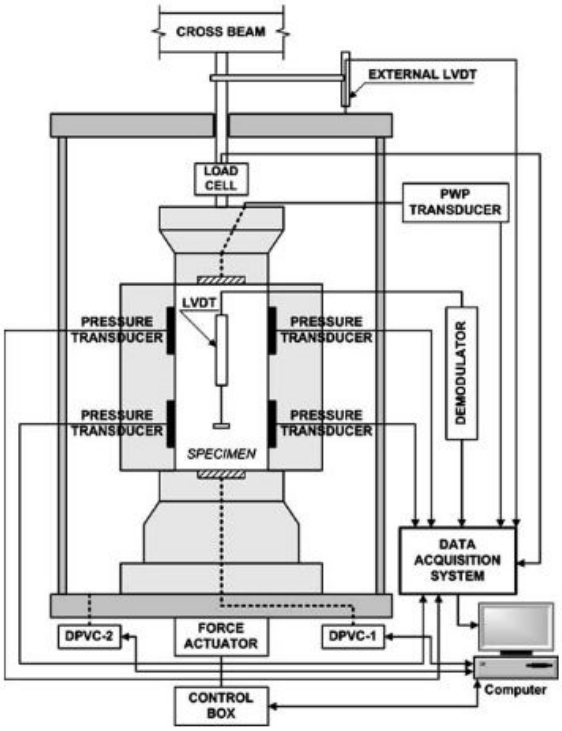

Figure 2-14. Schematic of NTU plane strain device (Wanatowski 2005)

CHAPTER 3.

TESTING MATERIALS

3.1Silica Sand

All tests were performed using ASTM C778 graded silica sand. The grain size distribution of this sand is shown Figure 3-1. The silica sand has a mean grain size (D_{50}) of 0.36 mm, a coefficient of uniformity (C_u) of 1.5, coefficient of curvature of (C_c) of 0.95, and a fines content of 0.1%. According to Unified Soil Classification System, this sand is classified as a poorly graded clean sand (ASTM D2487). The maximum (e_{max}) and minimum (e_{min}) void ratios were 0.80 and 0.50 as determined by ASTM D4254 and ASTM D4253. A summary of the properties of the sand is given in Table 3-1.

Table 3-1. Summary of sand properties

Specific Gravity	Mean Grain Size D_{50}	Coefficient of Uniformity C_u	Coefficient of Curvature C_c	Maximum Void Ratio e_{max}	Minimum Void Ratio e_{min}	Fines Content %
2.65	0.37	1.50	0.95	0.80	0.50	0.10

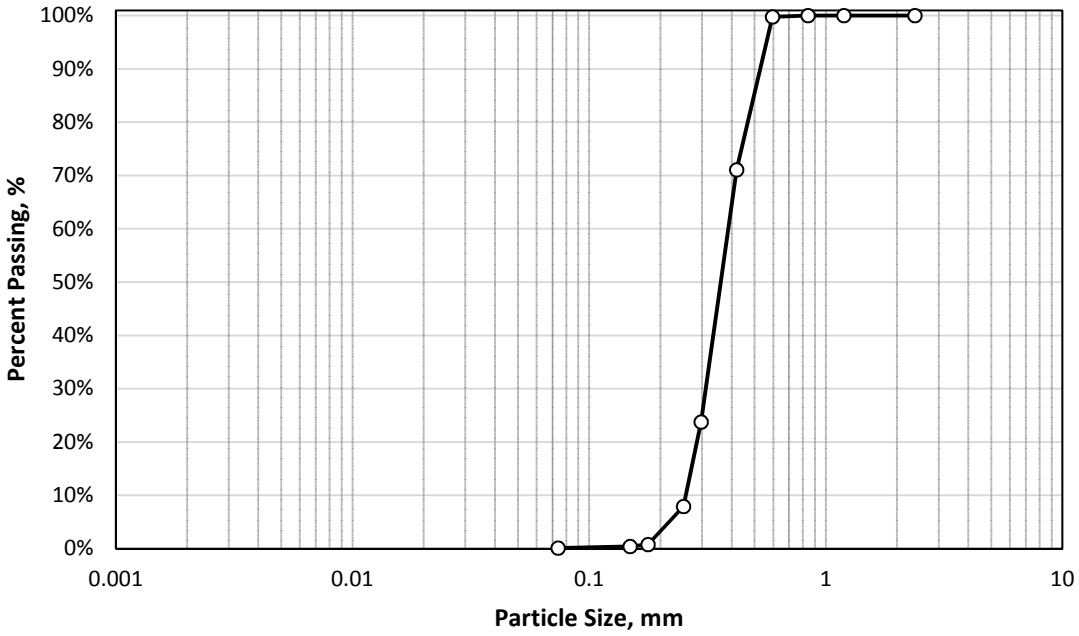

Figure 3-1.Grain size distribution of silica sand

3.2Denitrifying Bacteria

The denitrifying bacteria used in this study were collected from soil samples sampled at various sites across Iowa State University's campus in Ames, IA. Figure 3-2, shows an example of colonies of denitrifying bacteria on an agar plate. Since the soil contains many different types of bacteria, it was important to isolate the denitrifying bacteria from the other strains of bacteria in the soil. This isolation began by providing an environment favorable to the denitrifying bacteria. To produce a favorable environment for the denitrifying bacteria, a nutrient solution was prepared. The nutrient solution consisted of 1.01 g/L of potassium nitrate (KNO_3), 0.5 g/L ethanol (C_2H_5OH), 0.12 g/L ammonium chloride (NH_4Cl), 0.75 g/L of monopotassium phosphate (KH_2PO_4), 2.5 g/L of dipotassium phosphate (K_2HPO_4), 0.1 g/L of magnesium sulfate heptahydrate ($MgSO_4 \cdot 7H_2O$), 0.01 g/L

of ferrous sulfate heptahydrate ($FeSO_4 \cdot 7H_2O$), 0.015 g/L calcium chloride dehydrate ($CaCl_2 \cdot 2H_2O$), and 1 mL/L of trace element (DSMZ SL-12 B). All of the above ingredients were mixed with 1 L of distilled water in order to produce a growth medium that was favorable to the denitrifying bacteria.

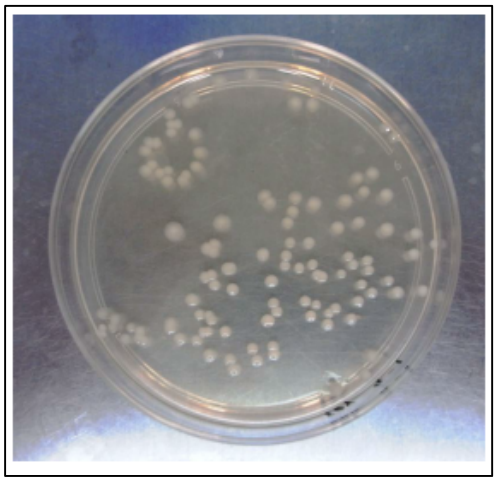

Figure 3-2.Colonies of denitrifying bacteria (He, 2013)

To isolate the denitrifying bacteria, three batch experiments were performed with the growth medium detailed above to favor the denitrifying bacteria. In the first batch, 50 grams of soil was mixed with the growth medium above in a 1 L glass bottle and placed on a shaker for 15 minutes. The liquid culture was purged with nitrogen gas and then transferred to a light-proof environment for 30 hours. After 30 hours, 200 mL of the first batch was mixed with 800 mL of growth medium which constituted the second batch. The process for the third batch was similar to that of the second batch. The third batch was kept in a refrigerator for up to two weeks as an enrichment culture for further use.

After obtaining the enrichment culture, the bacteria could be used in the gas generation tests and the triaxial tests. In order to do this, a bacteria solution was prepared

in a similar manner to that of the enrichment culture above. First, 1.8 liters of nutrient solution was prepared according the nutrient solution used above. The only major difference is that 0.66 g/L of glucose was used rather than 0.5 g/L of ethanol as the electron donor and carbon source. All of the other ingredients were prepared at the same concentration. Next, 200-300 mL of the enrichment culture was mixed in with the other ingredients and allowed to sit for a couple of days away from any light source. After a couple of days, many gas bubbles could be seen inside the container.

To apply the bacteria to the sand specimens, a 1 L treatment solution was prepared. The treatment solutions consisted of 80% by volume of nutrient solution with varying concentrations of potassium nitrate and glucose and mixed with 20% by volume of the enrichment culture. By varying the amount of nitrate, the amount of gas produced by the denitrifying bacteria could be controlled quite accurately. The mass ratio of carbon to nitrogen (C/N) is very important and for all bacteria treated samples, a C/N ratio of 2.22 was used. This ensured that enough carbon was available for the denitrification process and that the nitrogen source was the limiting factor. A C/N of 2.2 was also used in producing the enrichment culture as well.

CHAPTER 4.

TRIAXIAL TESTS

4.1Testing Equipment

This section describes the GeoTAC TruePath™ Automated Stress path System used in this study. The GeoTAC TruePath™ system consists of an axial load frame, external load cell, a triaxial cell, two pressure-volume flow pumps, an external LVDT, pressure sensors, data acquisition, control hardware, and control software (see Figure 4-1). The software was provided by Trautwein Soil Testing Equipment of Houston, Texas.

The software included with the GeoTAC system included control programs for each stage of a triaxial test including: saturation, consolidation, and shearing for both undrained and drained conditions. The software also included packages for isotropic, anisotropic, and K_0 consolidation. This study utilized the isotropic and K_0 consolidation control programs.

Isotropic consolidation was achieved by holding the backpressure constant while increasing the cell pressure until the effective consolidation pressure was reached. Under isotropic stress conditions, the stresses on the sample is the same in every direction. This means that at the beginning of the shearing stage, there is no shear stresses applied to the sample. The volume change during consolidation was recorded by the pressure volume controllers.

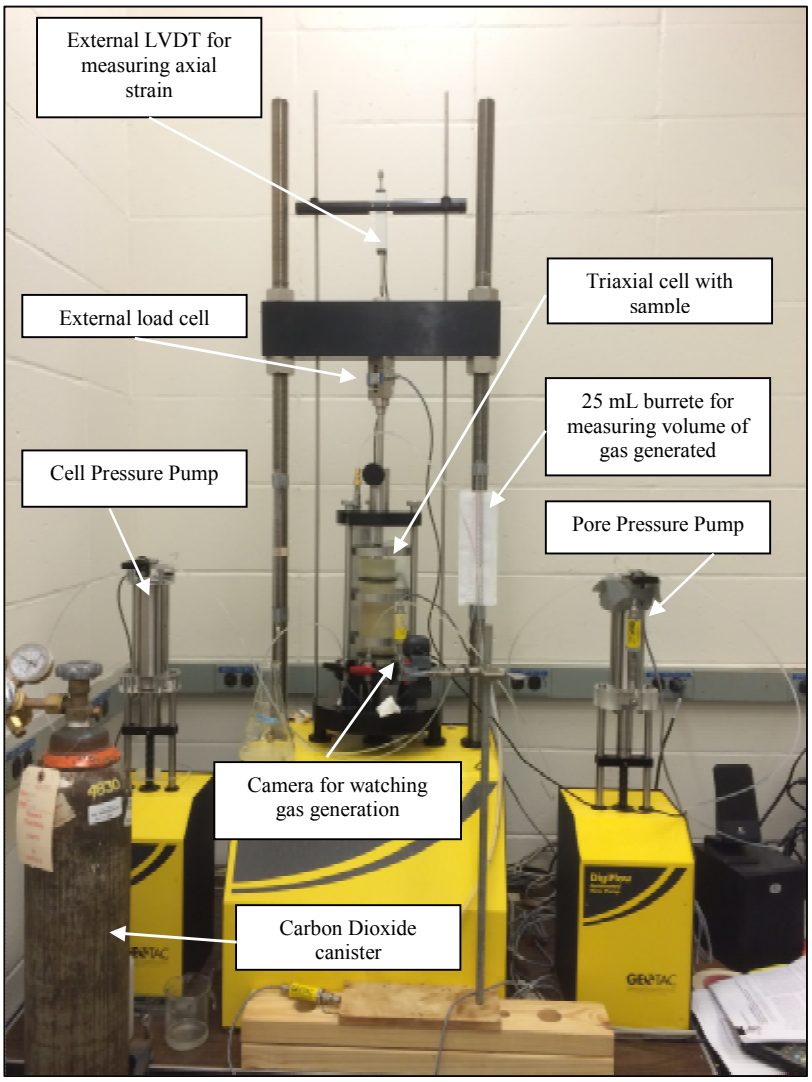

Figure 4-1.GeoTAC triaxial system

Under K_0 consolidation, an axial load is applied to the specimen in addition to the cell pressure. This induces shear stresses on the specimen prior to the shearing stage. The K_0 condition was imposed via the software by subjecting the specimen to a constant rate of deformation and extracting the pore water at a rate equal to the sample cross-sectional area times the deformation rate (Trautwein 2004).

$$d\varepsilon_v = A_c * d\varepsilon_1 \tag{10}$$

where $d\varepsilon_v$ is the volumetric strain, A_c is cross-sectional area, and $d\varepsilon_1$ is the axial strain (load frame displacement). During this process, the cell pressure was increased to keep the excess pore pressure equal to zero. The at rest earth pressure coefficient K_0, was determined with the following equation using the effective stresses at the end of consolidation.

$$K_0 = \frac{\sigma'_3}{\sigma'_1} \tag{11}$$

where σ'_1 is the vertical effective stress and σ'_3 is the radial effective stress.

4.2Testing Procedures

The following sections detail the testing procedures used for all of the triaxial tests. Two types of specimens were prepared: a fully saturated sample and a sample flushed the denitrifying bacteria solution. The testing procedures are outlined below.

4.2.1Sample preparation

The samples used in this study for triaxial tests were prepared using the moist tamping (MT) method. Samples were classified by relative density according to the classification system in Table 4-1.

Table 4-1. Classification based on relative density

Relative Density Dr (%)	Classification*
≤ 15	Very Loose
15 - 35	Loose
35 - 50	Medium Loose
50 - 65	Medium Dense
65 - 85	Dense
85 - 100	Very Dense

*After Skempton (1986)

The moist tamping method was employed to create loose sand samples. First, an oven dried amount of sand was prepared and mixed with 5% of de-aired water before being placed in the mold. Once the mold was assembled, the sand was placed and compacted in five layers. An image of the two part split-mold is shown in Figure 4-2. The height of each layer was carefully controlled so that a uniform loose sand specimen could be made. Once the top cap was assembled, a small suction of 10 kPa was applied through the use of a vacuum pump. The mold was then disassembled and the dimensions of the specimen were taken and the initial void ratio (e_o) was calculated. The cell was then assembled and filled with distilled water.

Figure 4-2.Two part split-mold used for preparation of triaxial samples

4.2.2Saturation

After filling the cell with distilled water, a cell pressure of 10 kPa was applied. All specimens were then flushed with carbon dioxide gas for 15-20 minutes so that lower backpressures could be used for saturation since carbon dioxide is more readily dissolved in water than air. For saturated samples, the sand was continuously flushed with de-aired water under a head of 0.5 m for 60 minutes. Bacteria treated samples were flushed with the bacteria solution under the same head and for the same length of time as for untreated samples. This process produced samples with initial B-values of 0.9 and above and were therefore assumed to be fully saturated. A backpressure of 100 kPa was applied to all samples.

For bacteria treated samples, the backpressure was increased to 100 kPa once the denitrification process was complete. The denitrification process was monitored by measuring the volume change after flushing via a burette attached to the top of the sample. This process is shown in Figure 4-3. A camera was set up to watch the volume change and was set to take pictures every 60 minutes through the use of a personal computer. When no further volume change was observed over a period of 1 hour, the reaction was assumed to be complete. Since the denitrification can be delayed by light, aluminum foil was used to block the light from affecting the growth of the bacteria.

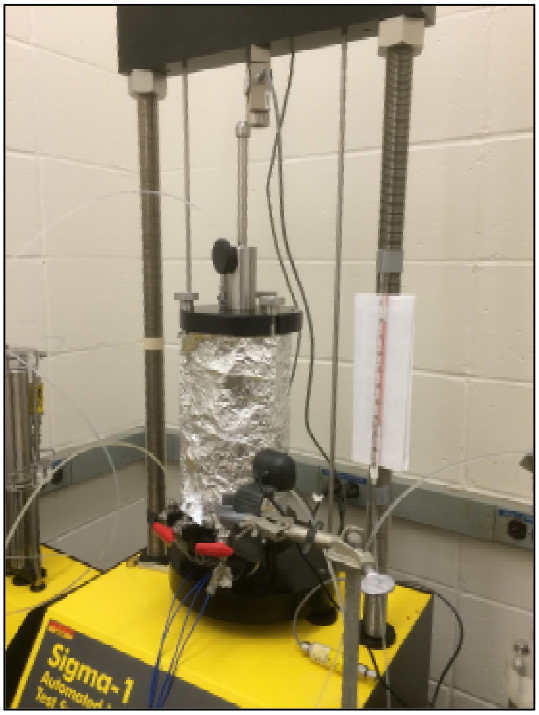

Figure 4-3.Monitoring of denitrification process in triaxial tests

4.2.3Consolidation & Shearing

4.2.3.1Isotropic Consolidation

All isotropically consolidated specimens were isotropically consolidated to an effective stress of 100 kPa. A stress rate of 200 kPa/hour was used during consolidation. Once consolidation was complete, the samples were sheared without drainage at a strain rate of 6% per hour.

4.2.3.2K_0 Consolidation

All K_0 specimens were consolidated along the K_0 line to a vertical effective stress of 100 kPa. A strain rate of 2.5% per hour was used. The volume change during consolidation was recorded by the pressure/volume controllers and recorded. Once consolidation was complete, the samples were sheared without drainage at a strain rate of 6% per hour.

4.2.4Void Ratio Calculation

Void ratio plays a vital role in the behavior of sand. For clean sand samples to determine the void ratio, the mass of moist sand, moisture content, sample circumference, sample length, and membrane thickness were all measured after the sample preparation process was completed and before the assembling of the triaxial cell. The void ratio after consolidation was then calculated based upon the volume change recorded during the consolidation stage using the following equation.

$$e_c = \frac{V_v - \Delta V_c}{V_s} \tag{12}$$

where e_c is the void ratio after consolidation, V_v is the volume of voids, ΔV_c is the volume change during consolidation recorded by the pressure-volume controllers, and V_s is the volume of solids.

4.2.5Estimated Degree of Saturation

For microbially desaturated specimens, the degree of saturation was estimated based upon the measured gas produced during the denitrification process. However, since the gas was formed at atmospheric pressure (assumed to equal 101.3 kPa), the volume of gas after saturation to 100 kPa (absolute pressure 201.3) was significantly less. The gas was assumed to follow Boyle's law and the temperature was assumed to be constant. Thus the gas content could be estimated via equation (13).

$$V_2 = \frac{V_1 P_1}{P_2} \tag{13}$$

Where V_1 is the measured gas volume during denitrification process, P_1 is atmospheric pressure (101.3 kPa), and P_2 is the pressure after saturation (100+101.3=201.3 kPa). Assumptions made during this calculation are that all the gas generated during the denitrification process was nitrogen, gas generated only within in the sample, and that none of the gas generated dissolved into solution.

4.3Results

4.3.1Testing Program

A summary of the triaxial testing program is given in Table 4-2. Series 1 consisted of isotropically consolidated triaxial tests with a relative density of around 19%. Series 2 consisted of K_0 consolidated specimens with a relative density of around 13%. Series 3 consisted of K_0 consolidated specimens with a relative density of near 19%. In each series, the amount of nitrate was varied in order to create varying degrees of saturation. For the rest of this chapter, the following parameters will be used in the analysis of the triaxial test results.

$$p' = \frac{1}{3}(\sigma_1' + 2\sigma_3') \quad (14)$$

$$q = (\sigma_1' - \sigma_3') \quad (15)$$

Where p' is the mean effective stress, σ_1' is the vertical effective stress, σ_3' is the radial effective stress, and q is the deviator stress. The definition of p' and q are different between Chapter 4 and Chapter 6.

Table 4-2. Triaxial testing program

Sample	Treatment (g/L of KNO_3)	Void ratio before consolidation	Void ratio after consolidation	Relative density after consolidation (%)	B-value (after Saturation)	Estimated Degree of Saturation	Undrained Shear Strength (kPa)
CIU1	0	0.771	0.749	17.0	0.99	100.0%	25.2
CIU2	1.52	0.757	0.742	19.3	0.55	95.2%	38.4
CIU3	2.27	0.757	0.740	20.0	0.42	92.5%	43.2
CIU4	3.03	0.758	0.745	18.3	0.39	89.1%	64.8
CK_0U1	0	0.779	0.767	11.1	0.99	100.0%	26.5
CK_0U2	0.76	0.780	0.767	11.1	0.73	97.1%	26.1
CK_0U3	1.52	0.779	0.765	11.6	0.54	94.4%	25.8
CK_0U4	3.03	0.778	0.763	12.2	0.44	90.9%	25.9
CK_0U5	0	0.758	0.746	18.1	0.99	100.0%	30.4
CK_0U6	3.03	0.756	0.744	18.6	0.40	89.5%	30.1
CK_0U7	4.04	0.756	0.743	19.0	0.35	87.5%	28.9

4.3.2Isotropically Consolidated Triaxial Tests

The undrained responses of the isotropically consolidated biogas desaturated loose sand are shown in Figure 4-4. All test conditions were kept the same including: the confining pressure, the effective consolidation pressure, void ratio, and sample preparation methods. The only major difference between the samples is the degree of saturation. As shown in Figure 4-4(a), the effective stress paths are very different. Figure 4-4(b) shows the shear stress plotted against the axial strain. Sample CIU1, which was fully saturated, exhibited the lowest shear strength and the highest excess pore pressure generation. The excess pore water pressure at the end of the test was around 87% of the confining pressure. As the degree of saturation decreased, the shear strength increased and the excess pore water pressures decreased. Sample CIU4 with a B-value of around 0.39 exhibited complete strain hardening with a maximum shear stress of over double that of sample CIU1 and an excess pore water pressure of around 30% of the confining pressure. The excess pore water pressure versus axial strain is shown in Figure 4-4(c).

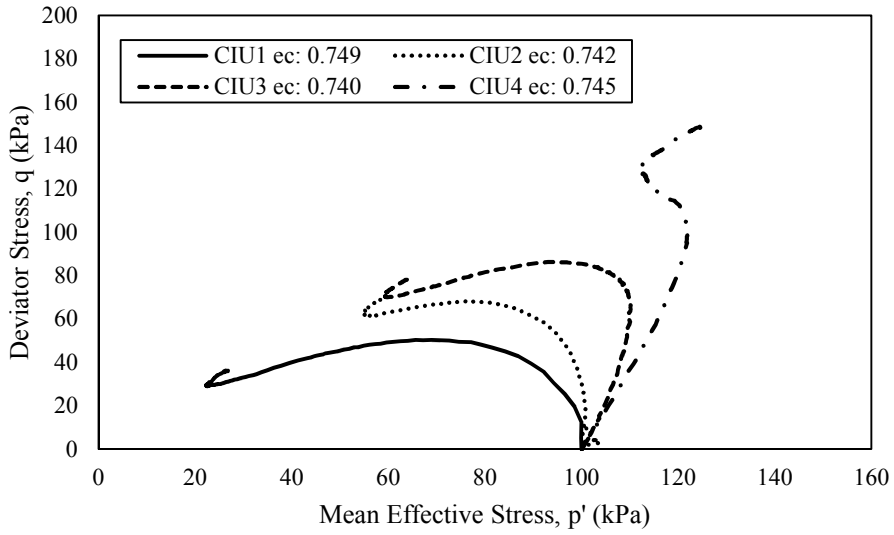

Figure 4-4(a). Effective stress paths

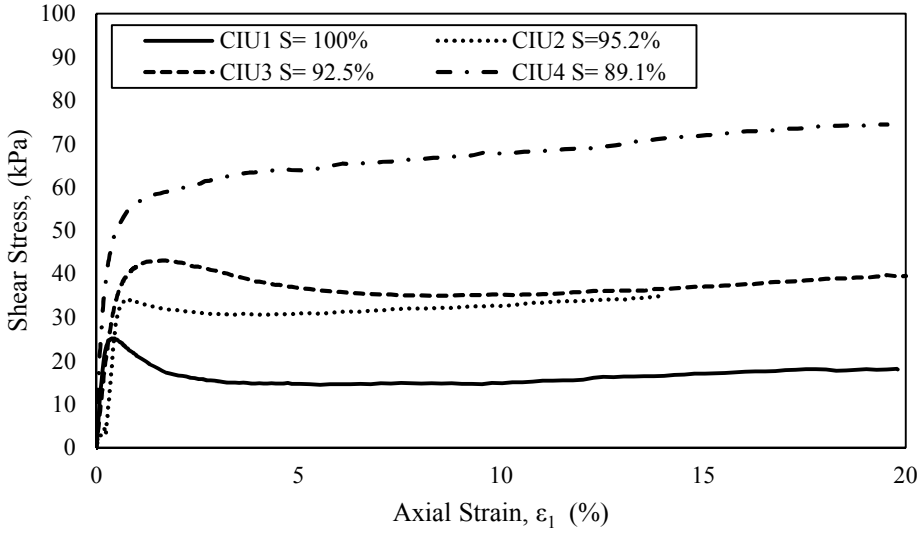

Figure 4-4(b). Shear stress versus axial strain

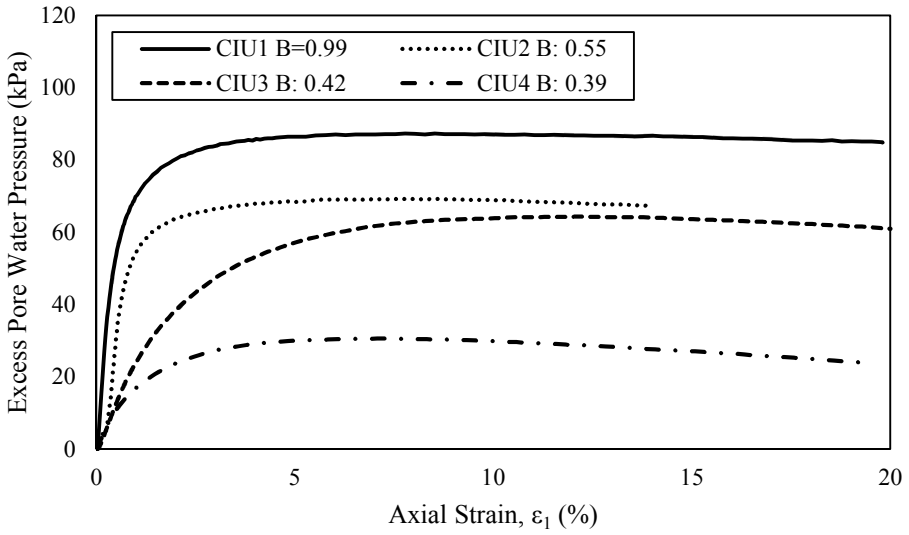

Figure 4-4(c). Excess pore water pressure versus axial strain

Figure 4-4.Results of the isotropically consolidated tests (a) effective stress paths; (b) shear stress versus axial strain; (c) excess pore water pressure versus axial strain

4.3.3K_0-consolidated Triaxial Tests

The undrained responses of the K_0 consolidated biogas desaturated loose sand at a relative density of around 11% is shown in Figure 4-5. With each sample test conditions were kept as close as possible. Due to the nature of K_0 consolidation program, the confining pressure may vary slightly from one sample to the next but the difference is negligible. The effective consolidation pressure, void ratio, and sample preparation methods were all kept similar. Again, the only major difference between the samples is the degree of saturation. As shown in the figures, there is little difference between the results of any of the tests. All tests exhibit a strain softening behavior with a maximum undrained shear strength of around 26 kPa. As shown in Figure 4-5, the excess pore pressure generation is similar regardless of the degree of saturation with the maximum pore water pressure being between 63-74% of the effective confining pressure.

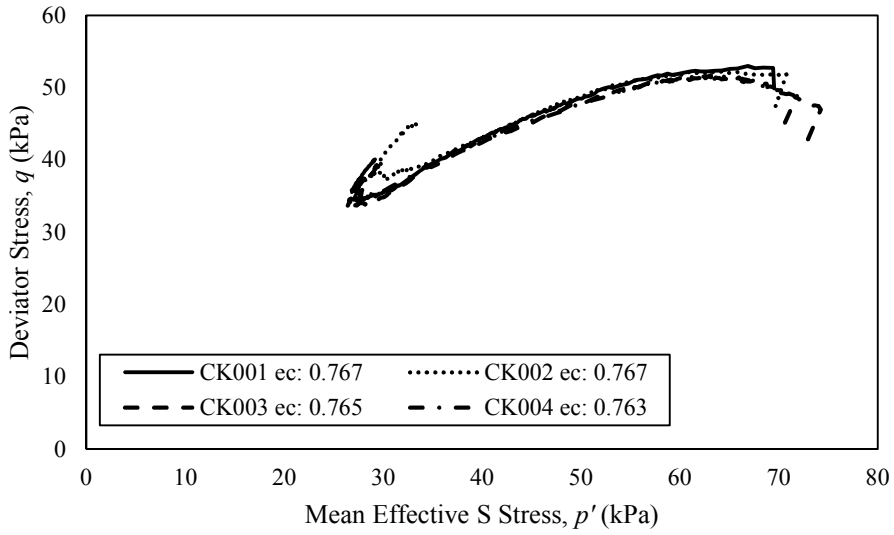

Figure 4-5(a).Effective stress paths

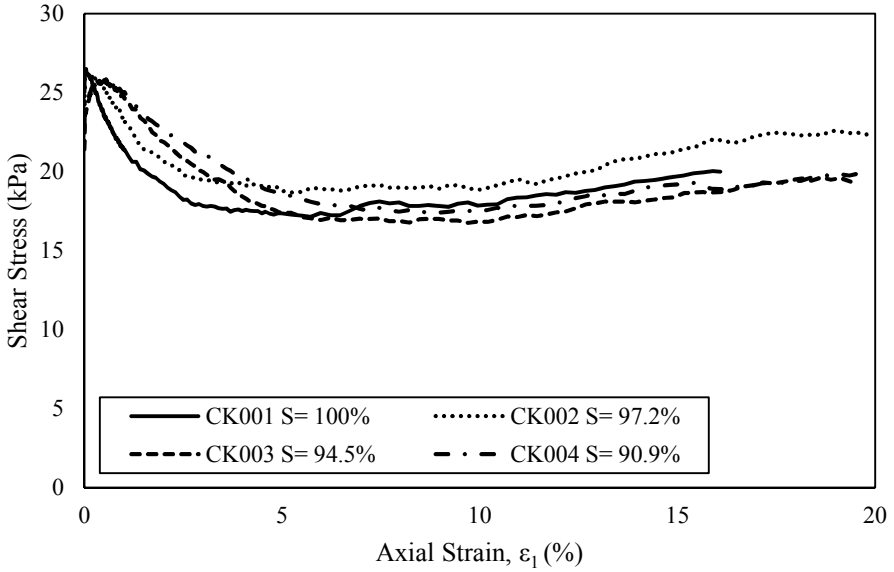

Figure 4-5(b). Shear stress versus axial strain

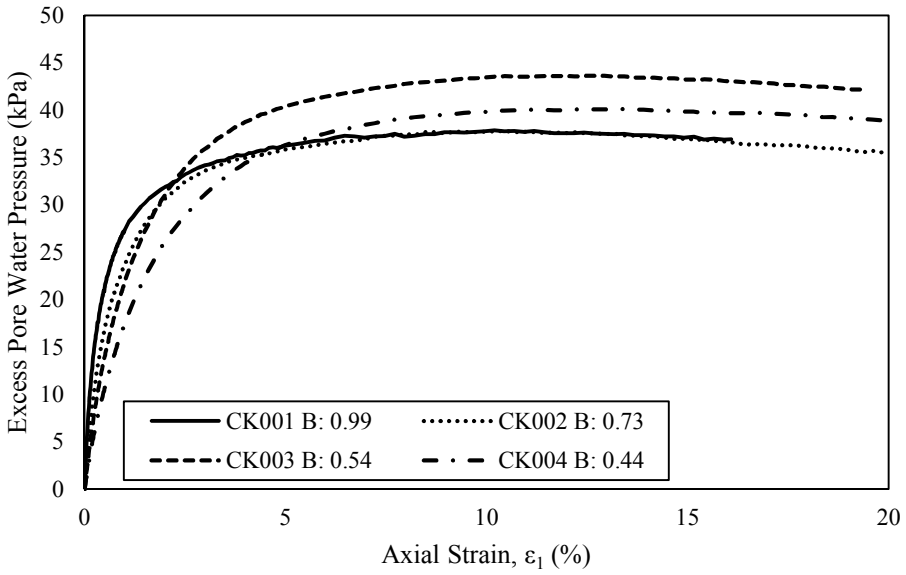

Figure 4-5(c). Excess pore water pressure versus axial strain

Figure 4-5.Test results for samples with a relative density around 11%; (a) effective stress paths; (b) stress-strain curves; (c) excess pore water pressure versus axial strain

The undrained responses of the K_0 consolidated biogas desaturated loose sand at a relative density of around 20% is shown in Figure 4-6. With each sample the test conditions were kept as close as possible. Again, due to the nature of K_0 consolidation program, the confining pressure may vary slightly from one sample to the next but the difference is negligible. The effective consolidation pressure, void ratio, and sample preparation methods were all kept similar. As with the previous tests, the only major difference between the samples is the degree of saturation. Figure 4-6(a), depicts the effective stress paths for samples CK_0U5, CK_0U6, and CK_0U7. As can be seen from Figure 4-6(a) the effective stress paths are quite similar regardless of Skempton B-value. In Figure 4-6(b), the maximum shear stress was held much longer for the partially saturated specimens as compared to the fully saturated specimen. As can be seen in Figure 4-6(c), the pore pressure

generation rate was slower for the partially saturated specimens. However, the maximum pore water pressure was about the same for every sample.

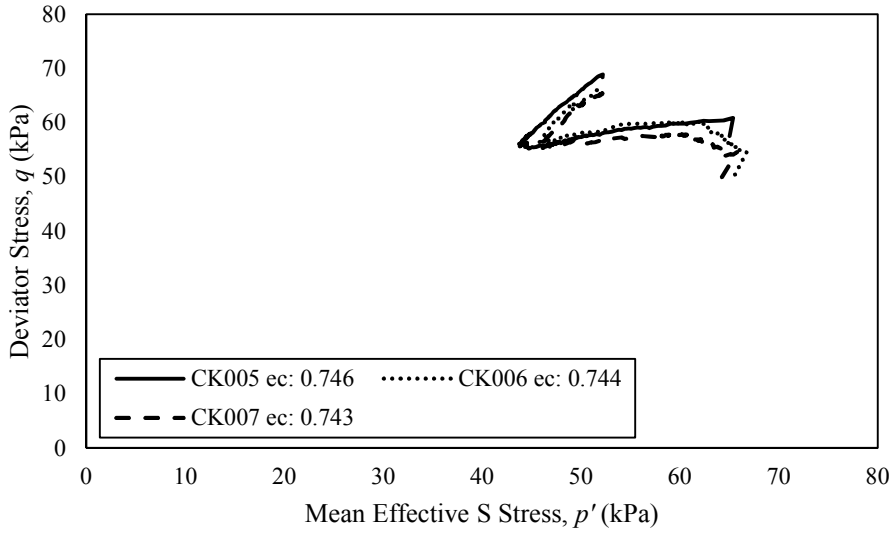

Figure 4-6(a).Shear stress versus axial strain

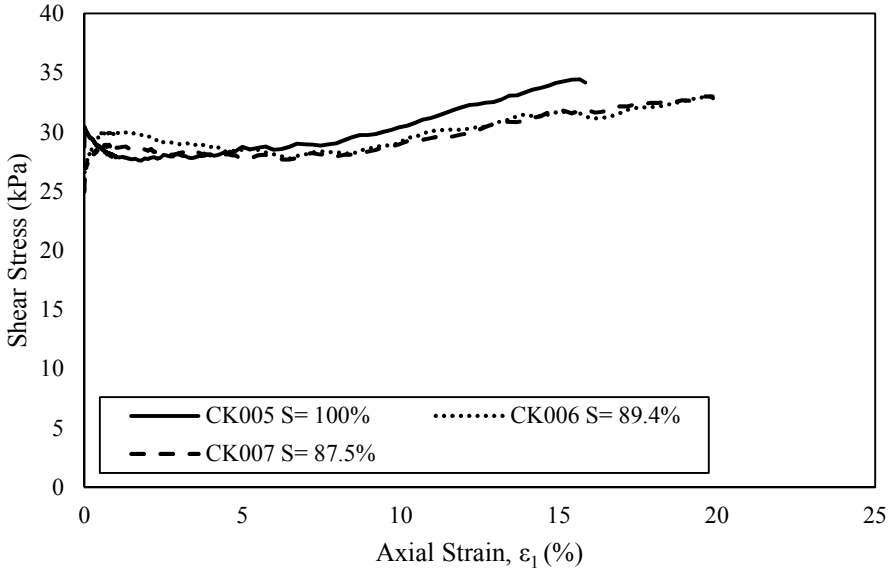

Figure 4-6(b).Shear stress versus axial strain

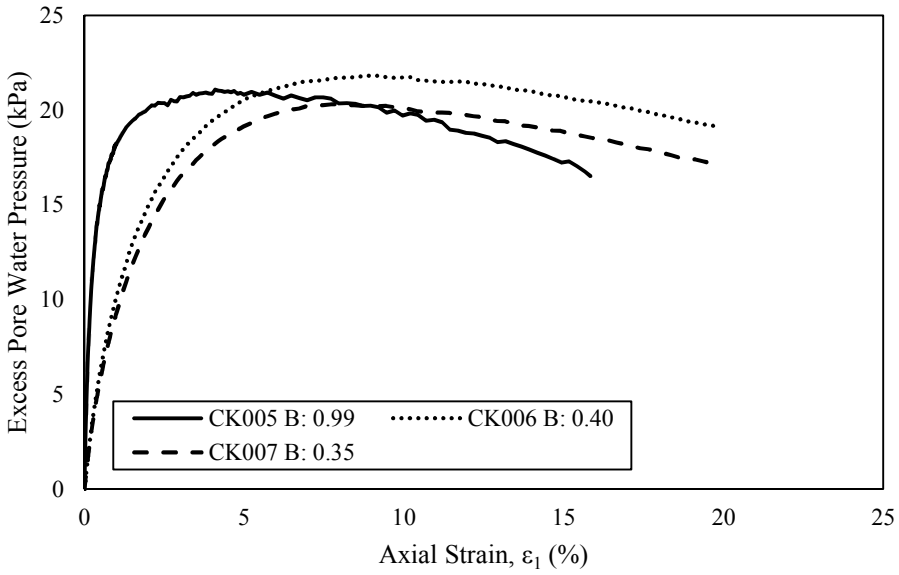

Figure 4-6(c). Excess pore water pressure versus axial strain

Figure 4-6.Undrained results for samples with relative density of around 20%; (a) effective stress paths; (b) stress strain curves; (c) excess pore water pressure versus axial strain

The results of all of the K_0 consolidated tests are given in Figure 4-7. Again, the degree of saturation seems to have less of an effect on the undrained behavior of biogas desaturated sand under K_0 conditions as opposed to isotropically consolidated samples. The presence of shear stress at the beginning of undrained shearing decreases the effect of the biogas on the undrained behavior of sand.

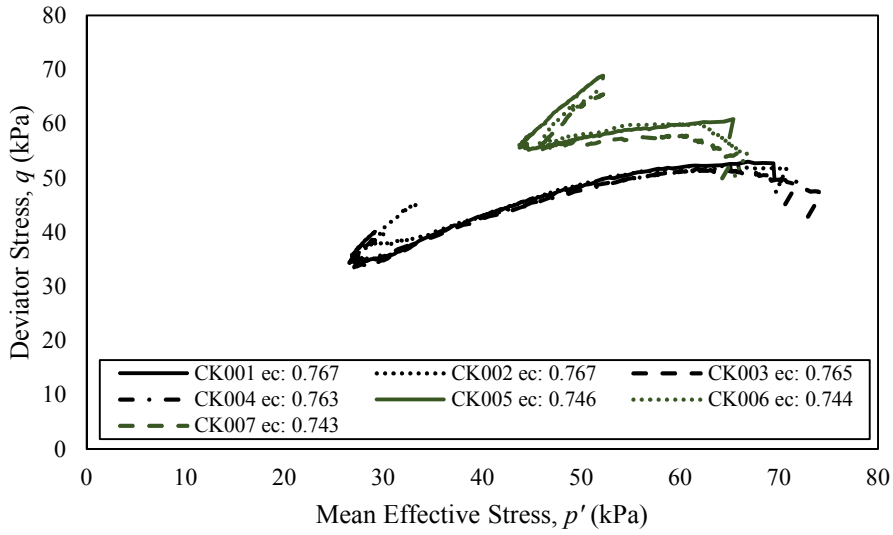

Figure 4-7(a).Effective stress paths

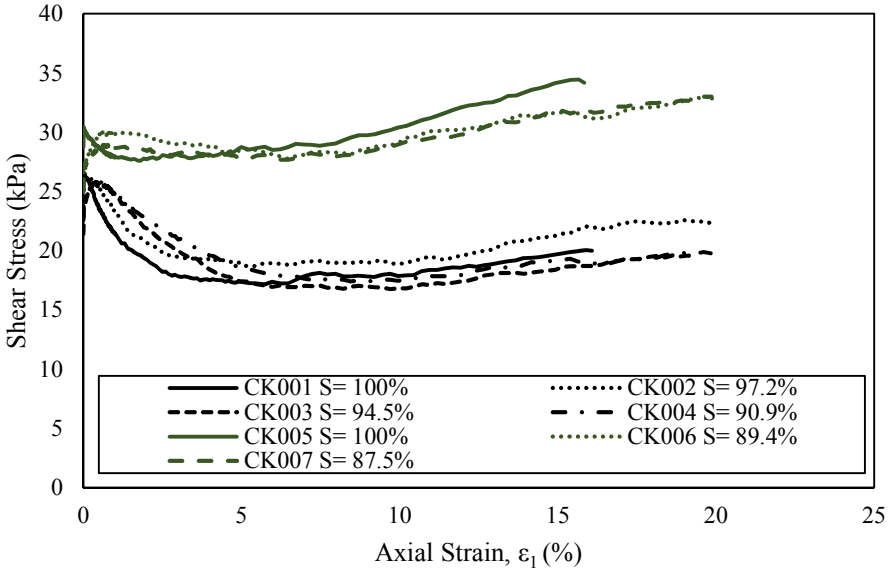

Figure 4-7(b).Stress-strain curves

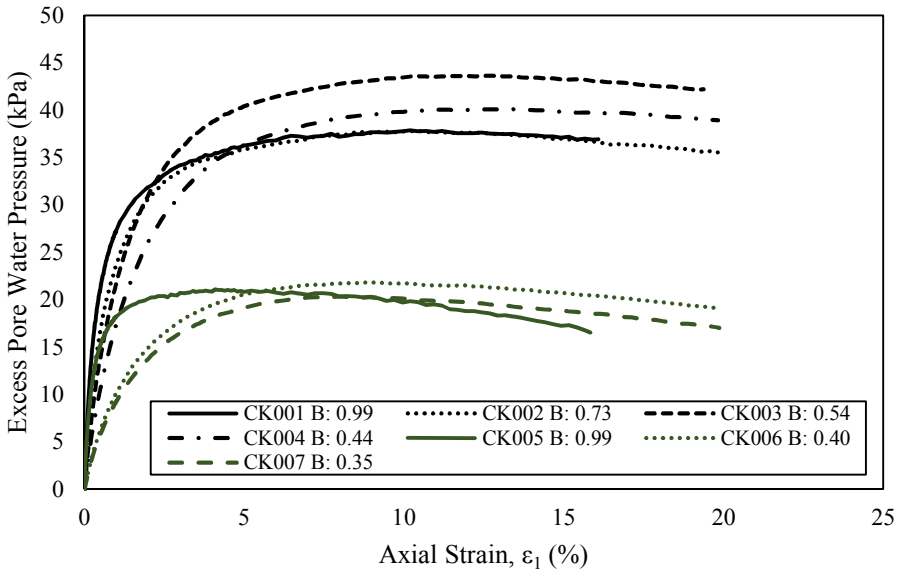

Figure 4-7(c).Excess pore water pressure versus axial strain

Figure 4-7.Comparison of all triaxial tests (a) effective stress paths; (b) stress-strain curves; (c) excess pore water pressure generation versus axial strain

4.4Conclusion

The results of isotropically consolidated and K_0 consolidated undrained triaxial tests have been presented in this chapter. The results of the isotropically consolidated samples showed that a loose sand can go from strain softening at a fully saturated state to that of strain hardening by changing the degree of saturation through the denitrification process. It was observed that by reducing the degree of saturation to around 89%, the peak shear stress can be increased from 25 kPa to a peak shear stress of 60 kPa under isotropic conditions. This is what has been reported in the literature review.

However, it was observed that samples consolidated along the K_0 line showed very little improvement compared to the isotropically consolidated samples. Samples that were K_0 consolidated showed similar peak shear strengths as well as similar amounts of pore

water pressure generation during undrained shearing regardless of the degree of saturation. It was observed that the peak shear stress of the microbially treated K_0 specimens was held constant for a longer time than the fully saturated K_0 specimens. It was also observed that the rate of pore water pressure generation decreased for partially saturated sand as compared to the fully saturated state. However, the magnitude of the peak shear stress and the maximum pore water pressure was similar in all K_0 consolidated tests regardless of the degree of saturation. As shown in Figure 4-7(b) and Figure 4-7(c), the development of the pore water pressure is delayed with decreasing B value. This delay may prevent a catastrophic failure caused by brittle behavior.

CHAPTER 5.

PERMEABILITY TESTS

5.1Introduction

The degree of saturation of soil can greatly affect the coefficient of permeability. This chapter comprises a simple study investigating the relationship between the degree of saturation and the coefficient of permeability of sand which has been treated with denitrifying bacteria. Several constant head permeability tests have been performed at varying degrees of saturation. The same sand and denitrifying bacteria were used as mentioned in chapter 3.

5.2Methods

5.2.1Constant Head Apparatus

To measure the effects of bio gas desaturation on the hydraulic conductivity, a constant head apparatus was constructed (Figure 5-1). The apparatus features a nominal 76 mm inner diameter acrylic tube 140 mm long and two globe valves. One valve was located at both the top and the bottom of the acrylic tube. A 15 mm tall layer of gravel was placed at the bottom of the acrylic tube. This allowed for free drainage through the bottom globe valve. Between the sand and the gravel layer, a permeable fabric was placed to prevent sand from flowing into the gravel layer. The change in head was measured using a measuring tape with an accuracy of +/- 0.5 mm. The change in head was measured as the difference between the water level in the acrylic tube and the elevation of the outlet tube.

The change in time was measured using a stopwatch with an accuracy of +/- 0.005 s. The amount of water flowing out was measured using a scale with an accuracy of 0.05 g. Constant head was achieved by pumping water into the top of the acrylic tube and letting the excess water drain out from the top valve. This ensured that during the test the hydraulic head was constant throughout the entire test.

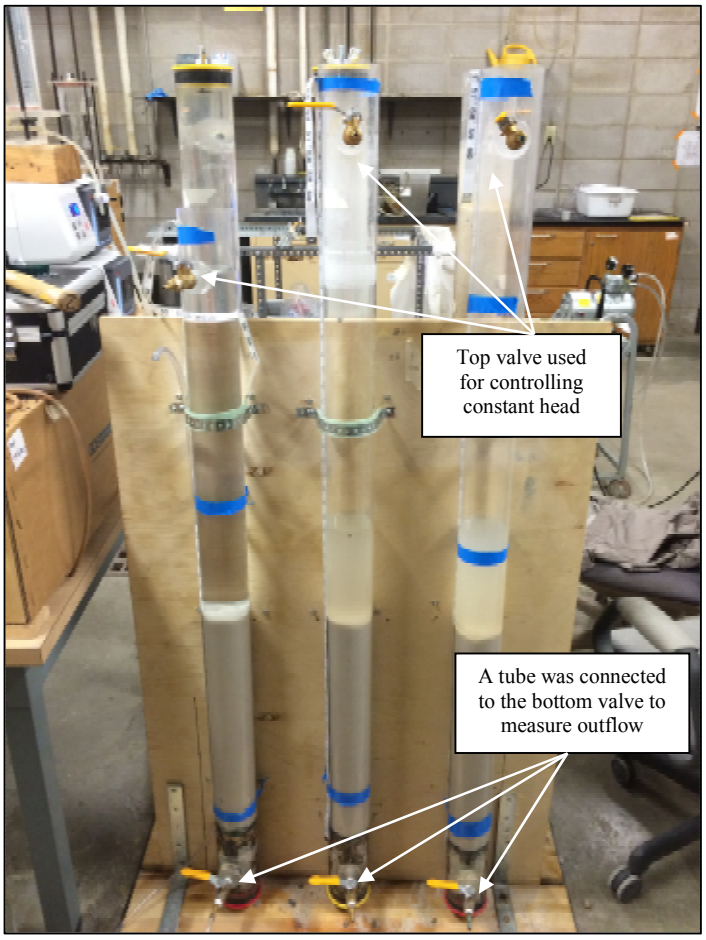

Figure 5-1.Apparatus for measuring hydraulic conductivity using constant head

5.2.2Sample Preparation

First, a layer of river gravel was placed at the bottom of the tube to a depth of around 15 cm. Next, a layer of pervious fabric was placed on top of the gravel layer to prevent sand from clogging the drain. It should be noted that the layer of gravel and the pervious layer of fabric would affect the measurement of permeability. Since the gravel and the filter have a higher permeability than the sand an effective permeability is measured. However, since the sand has the lowest permeability the effects of the gravel and the pervious layer are negligible. Next, a predetermined amount of dry sand was inserted into the acrylic tube via a PVC pipe. Sand was poured into the top of the PVC pipe until all of the sand had been placed in the PVC. Then, the PVC pipe was slowly lifted out of the acrylic tube and the dry sand was allowed to fall into place. The sand was then densified by tapping the side of the acrylic tube until the target void ratio was attained. This created a relative density of around 50%. Once the target density was reached, bacteria nutrient solution was flushed through the bottom valve and into the sample. The hydraulic gradient was carefully controlled as not to displace the sand particles. A hydraulic gradient of around 0.1 was used for the flushing. Once all of the nutrient had been flushed through the sample, the height of the water column was recorded. During the gas generation process, the water level in the tube rose over time due to the formation of nitrogen gas. The gas generation process took between 12 and 36 hours to complete depending on the initial concentration of nitrate. The change in volume was assumed to be the amount of gas generated in the sand. This volume was then used to estimate the reduction in the degree of saturation.

To determine the hydraulic conductivity (*k),* equation (16) for constant head was used.

$$k = \frac{V}{Ai\Delta t} \tag{16}$$

where k is the coefficient of permeability (cm/s), V is the volume of flow during a given time Δt (cm^3), A is the cross sectional area of the sample (cm^2), and i is the hydraulic gradient. An uncertainty analysis was performed in order to estimate the amount of error in the measurement of permeability. Based on the accuracy of the measurements, the uncertainty associated with this setup is around 1.0%. Therefore, this setup is adequate for the measurement of the coefficient of permeability in sand.

5.2.3Procedure

Once the gas generation process was complete, the acrylic tube was filled from the bottom to the top with distilled water and allowed to overflow through the top valve and into a 5 gallon bucket. Upward flow was used in order to help achieve a full saturation by dispelling air within the sand. After the tube was filled, the bottom valve was opened to allow the water to flow through the sample and up the tube where the water was to be collected. The height of the tube was positioned at a point 5 cm below the water level line. This achieved a hydraulic gradient of 0.1. The sample was allowed to drain for several minutes to achieve a steady state. Once the steady state was achieved and the water level at the top of the acrylic tube was constant, the samples were collected. For each test, a series of 5 samples were taken for a duration of 120 seconds. The samples were then weighed to determine the volume of the water. The density of water was assumed to be 1 g/cm^3. Knowing the sample diameter (assumed to be equal to the inside diameter of the tube), length, hydraulic gradient, and the amount of flow per unit time, the coefficient of permeability was determined according to equation 16. Figure 5-2 shows a schematic of the process outlined above.

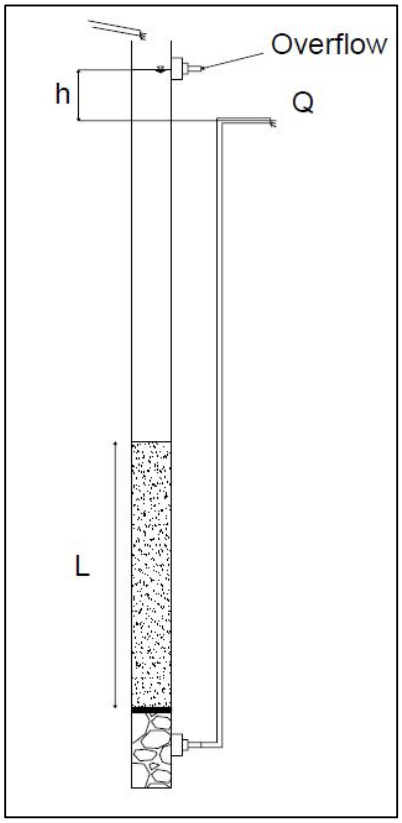

Figure 5-2.Schematic of constant head apparatus

5.3Results

A series of five constant head permeability tests were performed at a void ratio of 0.65 with the degree of saturation varying from 100% to 70.9%. From Figure 5-3, it can be seen that the gas production was completed within 48 hours. It was observed that as the initial concentration of potassium nitrate increases, the amount of gas produced increases accordingly except for the sample treated with 4 g/L of potassium nitrate. The degree of saturation was estimated based upon the amount of gas generated and the volume of voids within the sample.

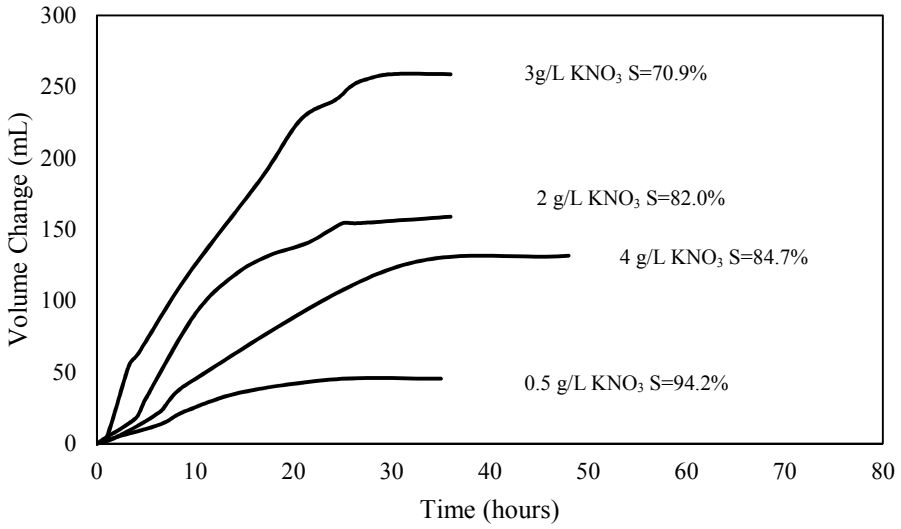

Figure 5-3.Gas generation of permeability tests

A summary of the results can be seen in Table 5-1. As can be seen in Figure 5-4, a fully saturated sand at a void ratio of 0.65 has a coefficient of permeability of 8.3 (10^{-4}) m/s. By reducing the degree of saturation to around 70%, the coefficient of permeability decreased to around 2.7 (10^{-4}) m/s. This is an overall reduction in the coefficient of permeability of around 67%.

Table 5-1. Results of constant head permeability test

Test	Void Ratio	Average k (10^{-4} m/s) i=0.2	Treatment (g/L of KNO3)	Volume Change (cm3)	Degree of Saturation
1	0.65	8.3	0.0	0.0	100%
2		7.6	0.50	49.9	94.2%
3		3.7	4.0*	131.7	84.7%
4		3.9	2.0	154.4	82.0%
5		2.7	3.0	249.7	70.9%

* Sample produced a smaller amount of gas than expected

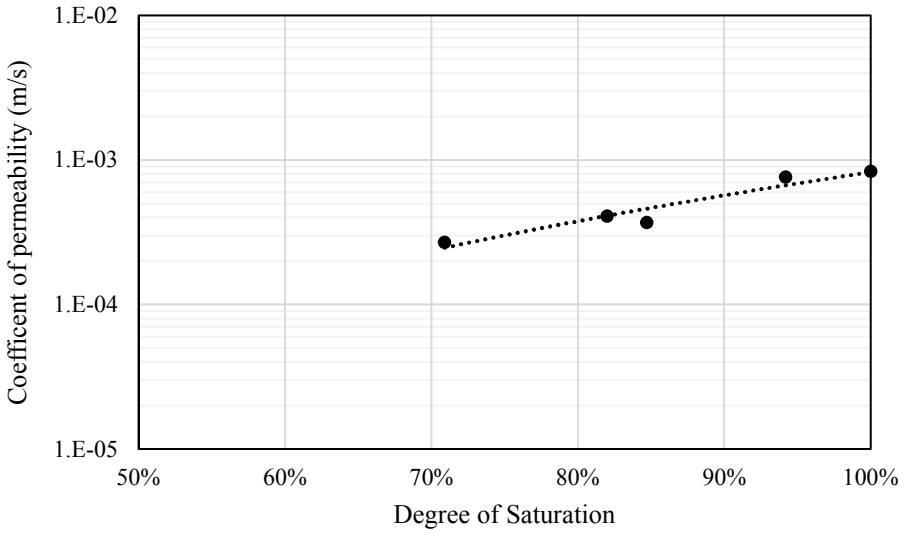

Figure 5-4.Relationship between degree of saturation and coefficient of permeability

5.4Discussion

According to Fredlund and Rahardjo (1993), Darcy's Law applies to the flow of water through a partially saturated soil. However, the coefficient of permeability will be lower than the fully saturated state for a given void ratio. For a saturated soil, the coefficient of permeability is mainly a function of the void ratio (Lambe and Whitman 1979).The coefficient of permeability for a partially saturated soil is a function of the degree of saturation or the volumetric water content as well as the void ratio. Water flow through a partially saturated soil can be visualized as only flowing through pore spaces that are filled with water. The volume available to water flow is taken up by the formation of the nitrogen gas bubbles produced by the denitrifying bacteria. As gas is formed, it displaces the water in the larger pores causing the water to flow through the smaller pores with increased tortuosity (Fredlund and Rahardjo 1993). The results above seem to agree with Fredlund

and Rhardjo (1993). As the degree of saturation was decreased from a fully saturated state to a degree of saturation of 70.9%, the coefficient of permeability decreased by 67%.

Fredlund and Rahardjo (1993) also proposed an equation in order to estimate the reduction in the coefficient of permeability for a clean sand (see equation 17).

$$k_{PS} = k_{FS} S_e^{\delta} \tag{17}$$

Where k_{PS} is the coefficient of permeability for a partially saturated sand, k_{FS} is the coefficient of permeability for a fully saturated sand, S_e is the effective degree of saturation, and δ has a value of 3 for clean sands. The equation for the effective degree of saturation is given in equation (18).

$$S_e = \frac{S - S_r}{1 - S_r} \tag{18}$$

Where S_e is the effective degree of saturation, S is the degree of saturation, and S_r is the residual degree of saturation at which a further reduction in matric suction does not significantly change the coefficient of permeability, k. Since matric suction was not measured in this study, the effective degree of saturation was assumed similar to the actual degree of saturation.

Using equation 17 and 18, a fully saturated sand with a coefficient of permeability of 8.3 (10^{-4}) decreased to a degree of saturation of 70.9 % one can expect the coefficient of permeability for a partially saturated sand to be around 2.96 (10^{-4}) m/s. While this value is slightly higher than the observed value, this relationship seems to agree with the results obtained for the constant head permeability tests performed in this chapter. Using the data, the residual degree of saturation can be calculated using equation 17 and 18. Using k_{PS} (2.7 (10^{-4}) m/s), k_{FS} (8.3 (10^{-4}) m/s), and δ (3) the effective degree of saturation can be

calculated as 68.8%. Using this calculated effective degree of saturation the residual degree of saturation can be determined using equation 18. From equation 18 the residual degree of saturation was found to be 6.7%.

5.5Conclusions

A series of five constant head permeability tests were presented in this chapter. The samples had the same density and a similar hydraulic gradient was applied to all samples. The only difference between the samples was the degree of saturation. From the results, it can be seen that with a treatment of 3 g/L of KNO_3 that the degree of saturation could be reduced by around 30% using the microbial denitrification method. This reduction in the degree of saturation reduced the measured coefficient of permeability from 8.3 (10^{-4}) m/s to 2.7 (10^{-4}) m/s. This equates to a reduction in the permeability of around 67%. In order to be used as a practical means for reducing the permeability of sands the reduction should be between 100 to 1000 times lower. Therefore, it can be concluded that the microbial denitrification method is not a practical method for reducing the permeability of clean sands.

CHAPTER 6.

PLANE STRAIN APPARATUS

6.1Introduction

The following sections describe the plane strain testing device developed in this study. The plane strain apparatus (PSA) was constructed to provide an advanced soil testing apparatus to the civil engineering department at Iowa State University. The benefits of the plane strain testing device include:

1) Stress conditions under plane strain are more representative of structures such as embankments, retaining walls, and slopes. Structures such as these can be closely approximated to the plane strain conditions.
2) This device allows for the measurement of "out-of-plane" stress via pressure transducers located within the rigid plates imposing the plane strain condition.
3) Free end technique allows for minimal friction between sample and rigid pieces. This allows for formation of shear band.

6.2Design

6.2.1Overview

The PSA is modeled after the device described by Wanatowski and Chu (2007). Figure 6-1 shows an overview of the plane strain apparatus described herein. The device consists of an axial load frame, triaxial cell, one submersible load cell, one submersible linear variable differential transformers (LVDT), one external LVDT, four soil pressure transducers, two GDS Advanced Pressure Volume Controllers (APVC), one pore pressure

sensor, and National instruments data acquisition hardware.A Visual Basic (vb.net) computer program was modified from an earlier version to control the GDS controllers as well as the data acquisition hardware.

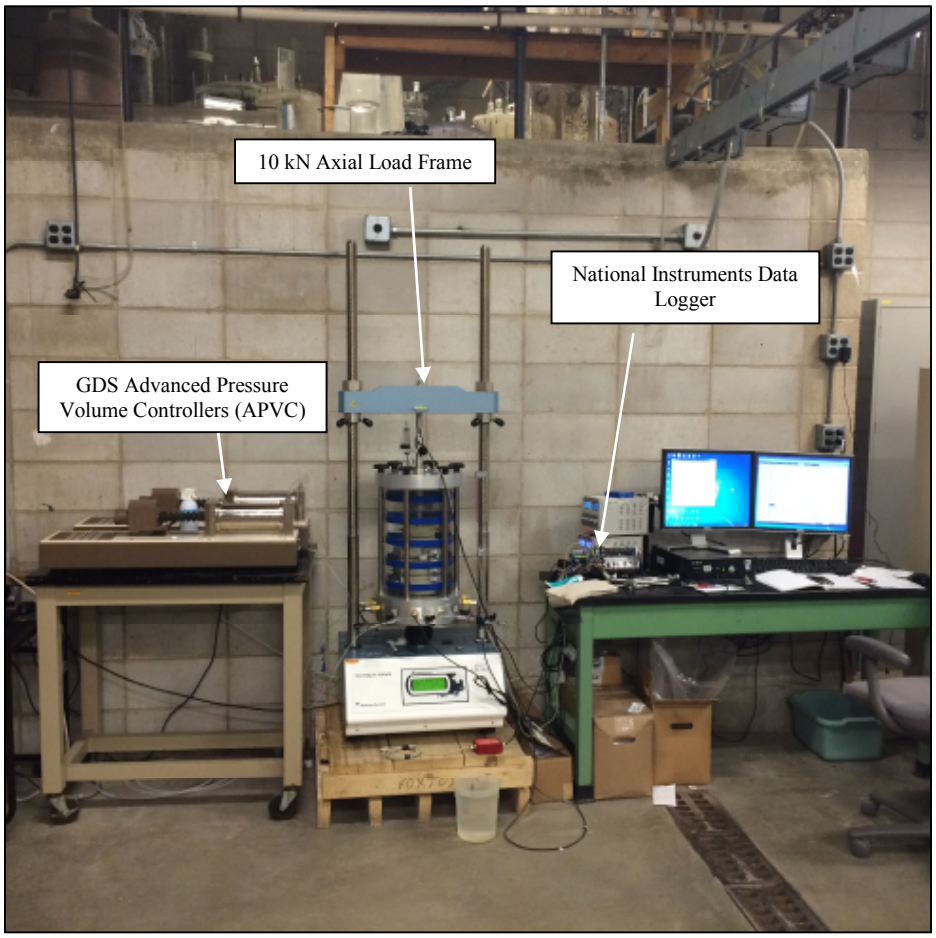

Figure 6-1.Overview of plane strain apparatus used in this study

The PSTA features a nominal 120 mm tall sample with a 60 x 60 mm prismatic cross-section. Two vertical plates were placed on either side of the prismatic specimen and were fixed in position by four horizontal steel tie rods. This prevented any lateral deformation along the direction of the tie rods which imposed the plane strain condition. All rigid platens were enlarged and lubricated using the free-end technique (Rowe and

Barden 1964). The free-end technique reduces boundary friction and delays the occurrence of non-homogenous deformations. One submersible LVDT was installed on one of the horizontal tie rods to measure small strains. Drainage was supplied by two 50.8 mm in diameter porous stones which were installed in both the bottom pedestal and top cap. Behind the porous stones was a 1/8" diameter hole leading to a stainless steel tube fitting. This connected the sample to the APVC controlling the pore pressure and volume inside the sample. The free ends consisted of a layer of high vacuum silicone grease and rubber membrane. This was done in order to reduce friction between the vertical platens and the sample. The same free end technique was also applied to the top and bottom of the sample to reduce the effects of the boundary conditions. Figure 6-2 depicts a plane strain sample as described above. The top cap, base pedestal, the lateral loading plates, as well as attachment pieces in order to complete the plane strain device were all fabricated for use in this study. The design of the top cap, base pedestal, and the lateral loading plates were adapted from the original NTU plane strain apparatus.

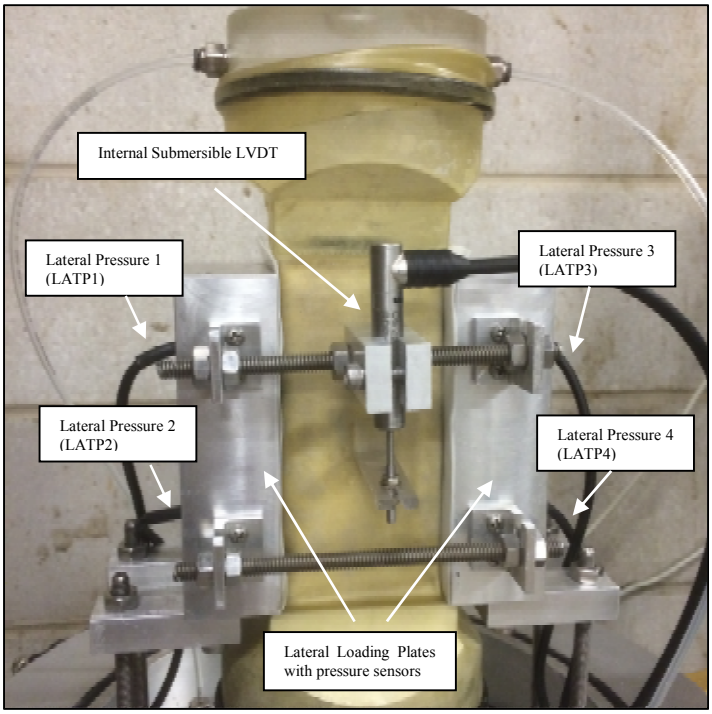

Figure 6-2.Diagram of contents inside plane strain cell

Embedded in each of the vertical plates were two submersible elevated-diaphragm type pressure transducers which were used to measure the lateral stress (σ_2) during consolidation and shearing (see Figure 6-3). Two transducers were installed in each plate so that the stress distribution between the top and bottom of the sample could be measured. These pressure cells were purchased from Kyowa Electronic Instrument Co. and had a capacity of 1,000 kPa with an accuracy of 0.01 kPa. The diameter of the transducers and the elevated diaphragm was 30mm and 23 mm respectively. The sensors were calibrated using a triaxial cell and a calibrated GDS controller. The submersible LVDT was purchased from RDP and had a linear range of +/- 5mm. The submersible LVDT was excited with 5V DC from a variable power supply. An external LVDT was also used to measure axial deformation once the submersible LVDTs ran out of range. The external LVDT was

excited by 10 volt DC. A summary of the calibration results can be seen in Table 6-1. From the results, all sensors exhibit exceptional linearity from 0 to 800 kPa.

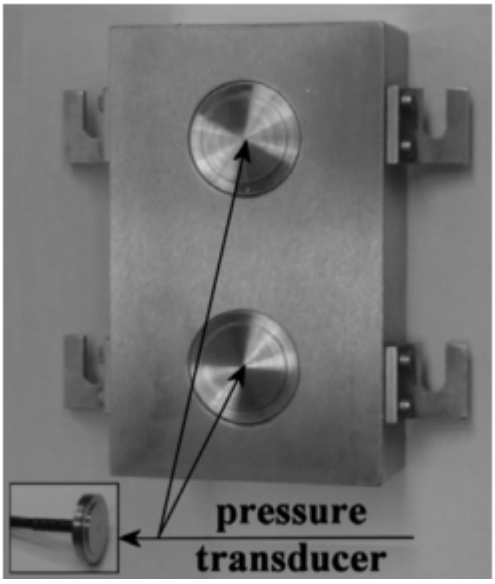

Figure 6-3.Lateral loading plate used to measure out of plane stress (after Wanatowski 2005)

Table 6-1. Summary of sensor calibration

Sensor	S/N	Calibration Coefficient (Unit/Volt)	Coefficient of Linearity	Supply Voltage
External LVDT (mm)	14005173	5.14403	0.9999	10 V DC
Load Cell (kN)	42818	451.3043	-	
Pore Pressure (kPa)	GS4200	10000	0.9997	
Lateral Pressure Transducer 1 (LATP1) (kPa)	GG1720002	-3968805	0.9999	2.5 V DC
LATP 2 (kPa)	GG1720004	-3863776	0.9999	
LATP 3 (kPa)	GH0690001	-3878239	0.9999	
LATP 4 (kPa)	GG1720001	-3836184	0.9999	

6.2.2Control Program

6.2.2.1Overview

A computer control program was written to perform the strain path tests by controlling the ratio of volumetric strain and axial strain ($d\varepsilon_v/d\varepsilon_1$) to a specified value using Visual Studio 2010. A National Instruments® data logger was used to measure and record the outputs of the internal load cell, internal LVDT, external LVDT, and the soil pressure cells. The program then takes these readings and calculates the appropriate stresses and strains. This information is then used in the control program. The structural layout of the program is shown in Figure 6-4. The basics of the control program for the strain path tests is as follows:

1) Read internal and/or external LVDT and compute axial strain, ε_1
2) Calculate volumetric strain ε_v and the volume change of the sample
3) Send message to GDS controller to target the volume change found in step 2
4) Read all channels and record data to a text file and then go back to step 1

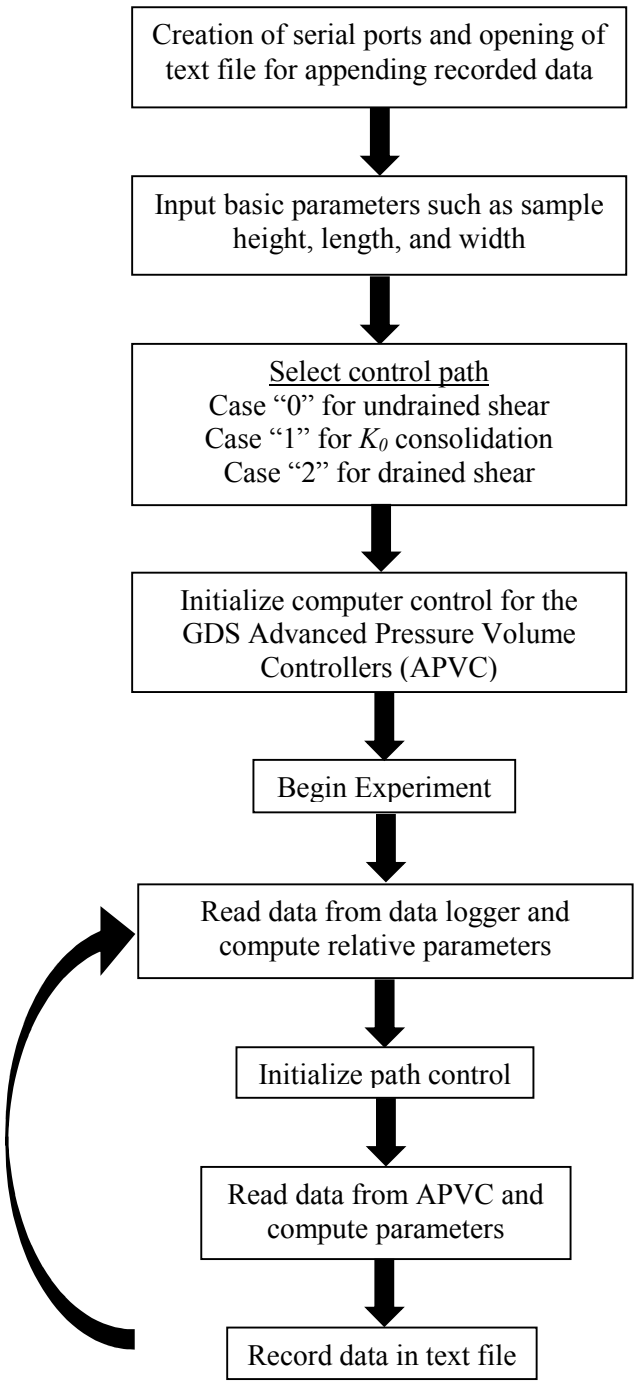

Figure 6-4.Structural layout of control program

6.2.2.2Program Design & Implementation

In order to read the data logger, a task was first created in Measurement Studio®. The task is shown in Figure 6-5. The task involved the setting up of sensor parameters for the all of the sensors to be read by the data logger. Timers were used in order to call the task created in measurement studio®. With every tick of the timer, the task was called and the data was retrieved from the data logger. This was set to occur at 5 second intervals throughout the test.

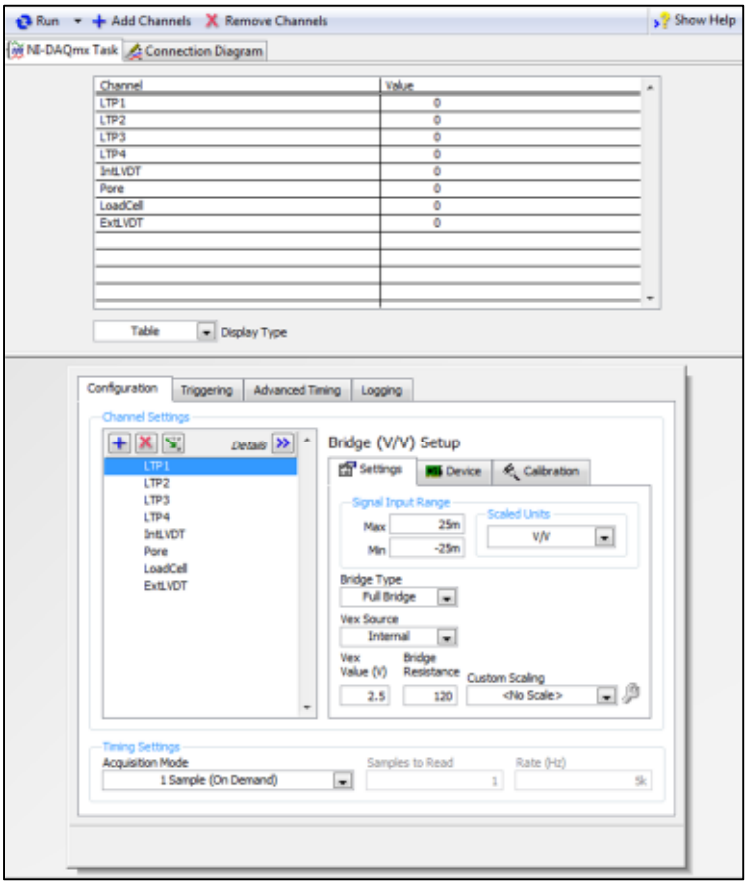

Figure 6-5.NI DAQmx task for reading channels

Upon opening the program the serial ports were created and opened in order to control the GDS controllers. The details of the serial port information is given in Table 6-2. Once the serial ports were created/opened, the program opens a text file called PST.txt where all of the data was recorded. The location of the file is as follows: C:\Users\Lab124\Desktop\PST.txt. Since the user does not have control over the file name or location, the program simply appends the new data to the old file so that old data is not lost. A warning appears upon the main form loading which warns the user to save the old file at another location prior to beginning the next test. Once these steps are completed the main form loads. This form is shown in Figure 6-6. The main form contains all of the input parameters and command buttons to initiate the recording of data for any stage of the test.

Table 6-2. Serial port settings

Serial Port	Serial Port Name	Baud Rate	Parity	Data Bits	Stop Bits
COM1	GDScell	4800	Odd	8	2
COM5	GDSpore	4800	Odd	8	2

The first step once the form loads is to input the testing parameters. Under the menu labeled “Setup” the form shown in Figure 6-7 opens up. Here the sample parameters such as width, length, height, and mass of dry sand can be input into the program. By entering the specific gravity of the soil, the void ratio before consolidation can be calculated. The user also has the option to use either the external or internal LVDT. If the internal LVDT is not used, then the control program uses the external LVDT throughout the entire consolidation and shearing process. If using the external LVDT, the loading piston must be seated prior to the beginning of consolidation. If the internal LVDT is checked, the internal LVDT is used for small strains to eliminate bedding errors as much as possible.

Once the axial strain deformation exceeds 1 mm, the program switches to using the external LVDT. Clicking “Okay” will record the data into the open text file and the file will close.

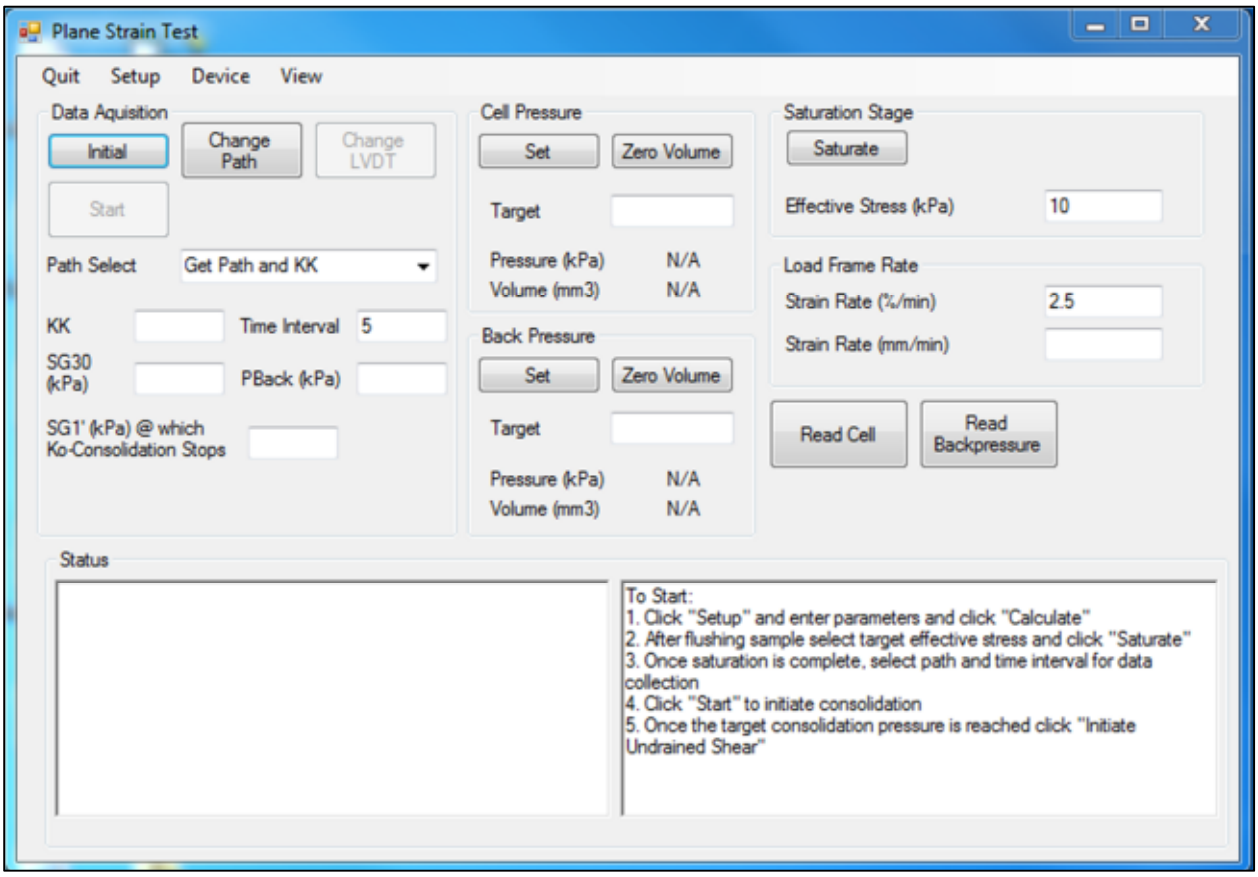

Figure 6-6.Program main menu

After the sample parameters and LVDT type are selected, the device menu opens back up. Next, the testing parameters should be selected. Clicking on the “Path Select” combo box opens a drop down menu where the user can select cases 0 to 2. Case 0, 1, and 2 is for undrained shear, K_0-consolidation, and a drained test respectively. At the beginning of each test case “1” was chosen. When case “1” is chosen a dialog box opens and allows the user to input the vertical effective stress (*SG1’*) at which K_0-consolidation stops. Once

the vertical effective stress reaches this value, the user must press the “Change Path” button. This button allows the user to change from consolidation to the shearing stage. Once this button is pressed, the timers controlling the program halt until the button is pressed again. Once the new path is selected, the user must press the same button again now labeled as “Continue”. This will resume all timers and data recording.

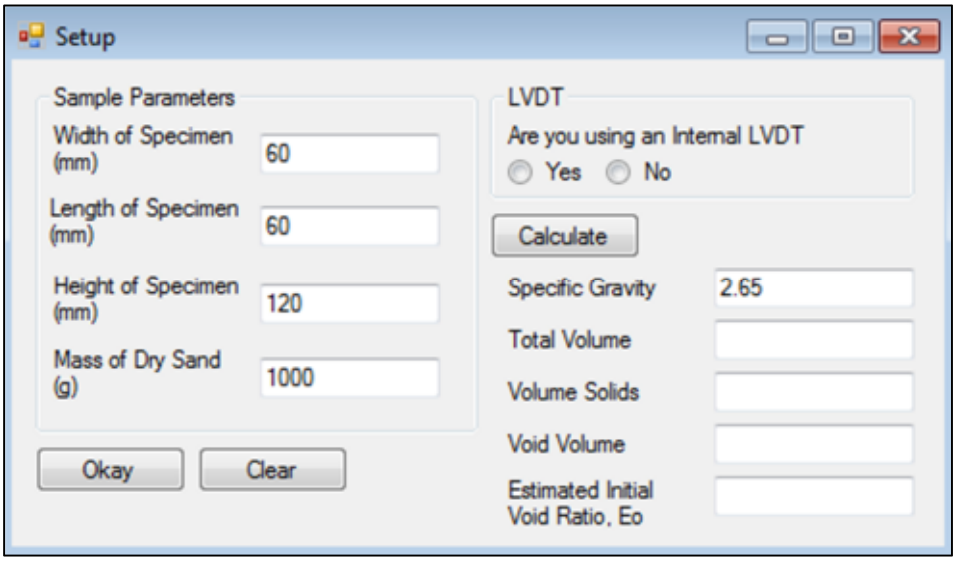

Figure 6-7.Setup menu of plane strain program

The next step is to verify that all of the equipment is in working order. This can be done by selecting the “Initial” button. This begins data logging without recording it to the file. The data that is read is then input into a table of initial values on the “Values” form (see Figure 6-8). The values form can be accessed under the “View” tab and selecting “Value”. This is only used to verify that the sensor are working prior to beginning the test. The button labeled “Stop” can be clicked in order to stop reading the data logger. The values form is also useful in seating the loading piston if using the external LVDT. Once the load reading begins increasing then the loading ram is seated onto the top cap and

consolidation can be initiated. Typically a load of 5-10 kPa was used to ensure that the piston was seated correctly. For a typical 60 mm x 60 mm sample this equates to an initial vertical stress of 1.4 - 2.7 kPa.

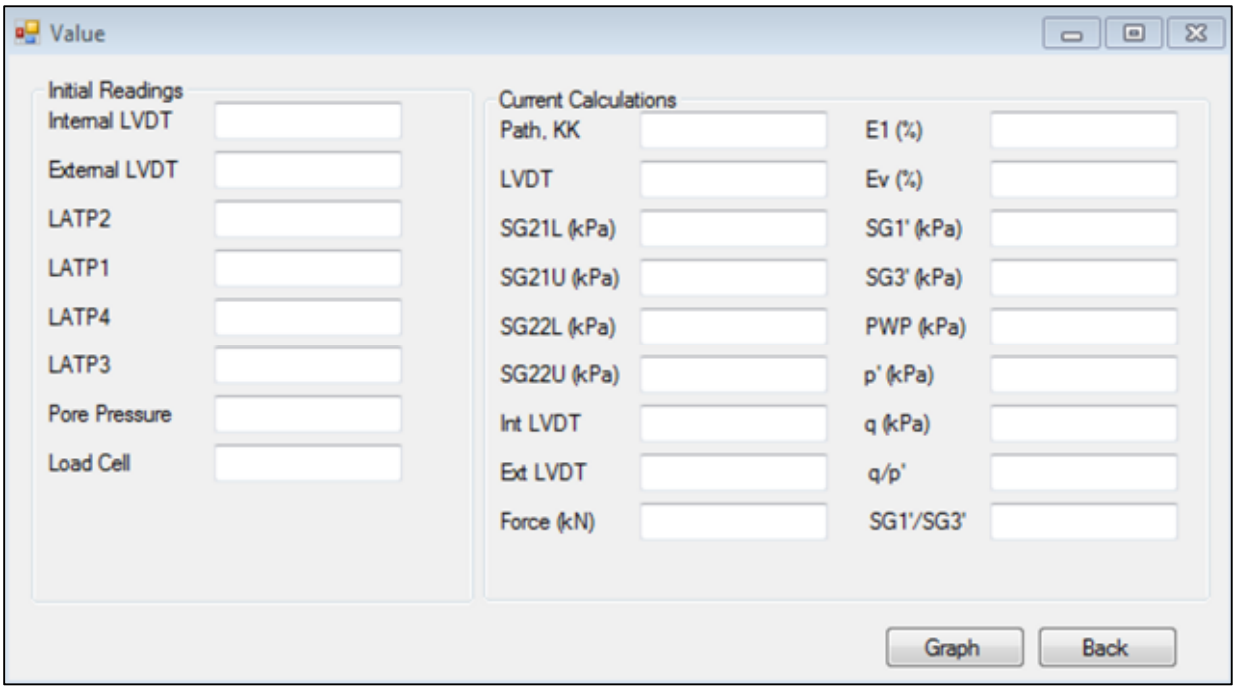

Figure 6-8.Form that shows current calculations and initial reading values during plane strain testing

After all the above steps are completed, the saturation stage can begin. In order to saturate the specimen, the user can select the desired effective stress during saturation. To start the saturation, the user must click the “Saturate” button. The control program for the saturation stage was quite simple. First, the cell pump was commanded to ramp to 310 kPa with increments of 1 kPa every 38 seconds. This allowed the back pressure to achieve a target of 310 kPa in about 190 minutes. By clicking the “Saturate” button, a timer begins commanding the AVDPC controlling the pore pressure to target the cell pressure minus the desired effective stress. To achieve a different back pressure or to change the timing of

the pressure increments, the subroutine for the back saturation stage must be rewritten as needed. To create new ramping settings, the user must define four items: timing between increments (ms or s), initial target pressure, final target pressure, and executing the command. The command to ramp the cell pressure is given like this using the COMM ports and a serial cable. See the manual for the GDS controllers for further information regarding this step.

Once the target back pressure has been reached, the consolidation stage can begin. It is important to note that the program only has the ability to control the GDS controllers. The program does not control the axial load frame during consolidation or shearing. The load frame must be monitored and controlled by the user manually. To initiate the consolidation stage, the first step is to calculate the appropriate deformation rate. The default strain rate is 2.5% per hour. For a 120 mm sample this equates to a deformation rate of 0.0500 mm/min. This can be entered into the axial load frame controller manually. Going back to the control program and prior to selecting “Start”, ensure that the sample dimensions and testing parameters have all been entered. Selecting “Start” imitates the control program for the consolidation and shearing portion of the test. The details of the control program are highlighted in the previous section (5.2.2.1). Lastly, start the axial load frame after the control program begins so that the initial states can be recorded. As mentioned earlier, once the target vertical effective stress has been reached, the user must manually switch the program to the shearing stage by selecting the “Change Path” button and choosing either the undrained case (0) or the drained case (2) under the path control dropdown menu. The test can be stopped at any time by clicking the “Stop” button and by manually turning off the axial load frame. An undrained test is achieved by targeting zero

volume change during shearing. For a drained test, a constant backpressure is used to alleviate any excess pore water pressure generation during shearing. The backpressure that is targeted is the final backpressure reading at the end of consolidation.

6.3Testing Procedure

6.3.1Sample Preparation

The sample preparation methods used in the Plane Strain tests were similar to that of the triaxial tests. A four part split-mold was designed and utilized in this study. The split-mold was made of aluminum with two brass hose barb fittings which allowed the mold to be attached to a vacuum pump. The split-mold was held together by 8 socket cap screws. This allowed the mold to be easily taken apart and removed from the sample after the preparation process was complete.

To prepare the sample, the desired amount of sand was mixed with 5% water by weight. The sand was thoroughly mixed and placed in 5 layers of equal height. Then, high vacuum grease was applied to the top cap and the top cap was placed on top of the sample. The membrane was then stretched onto the top cap and the O-rings were placed on the sample to create a water tight seal. The lateral loading plates were then placed flush against the sample and the tie rods were attached and tightened. Great care was taken to ensure that the loading platens were flush against the sample and that the tie rods were only tight enough to prevent lateral movement without damaging the sample.

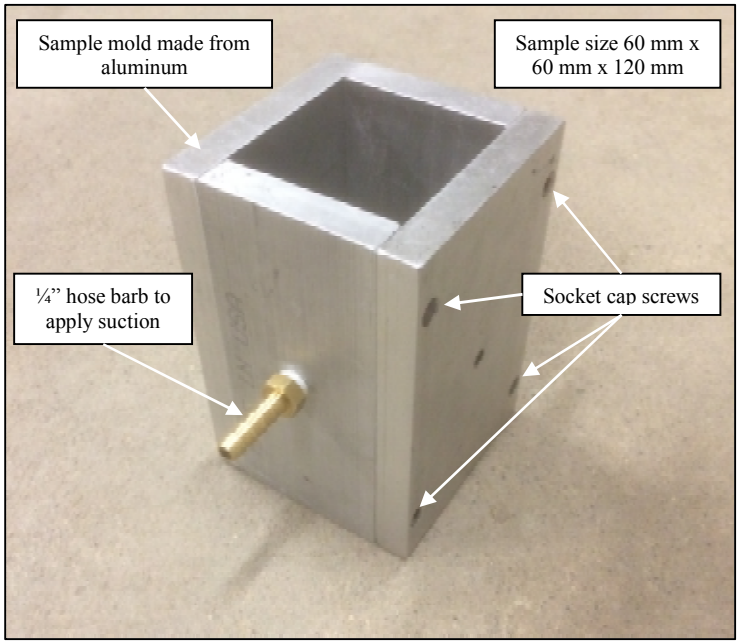

Figure 6-9.Four part aluminum split mold used for moist tamping sample preparation

Once the sample setup was complete, the cell was carefully placed over the sample making sure not to damage the sample in any way. The cell was then filled with distilled water and a cell pressure of 10 kPa was applied. Prior to saturation, carbon dioxide was flushed through the sample for 15-20 minutes to displace the air in the sample with a more readily dissolved gas. After flushing with CO_2, the sample was flushed with de-aired water under a head of 0.5 m for about 60 minutes. This process ensured that the degree of saturation was nearly 100% prior to the back saturation stage. Once flushing was complete, the backpressure was increased to 300 kPa to achieve full saturation.

6.3.2Consolidation & Shearing

Once the saturation stage was complete, the consolidation stage could begin. This was achieved through the use of the control program. A consolidation strain rate of 2.5%/hour was used. Once the vertical effective stress target had been reached, the

undrained shearing condition could be imposed manually by clicking the "change path" button. After clicking the change path button, the user should select either case "0" or case "2" for undrained and drained respectively. Since the axial load frame was not computer controlled, the shearing strain rate was the same as the consolidation rate of 2.5%/hour. The stress parameters used in the analysis throughout the rest of this chapter are as follows:

$$p' = \frac{1}{3}(\sigma_1' + \sigma_2' + \sigma_3') \tag{19}$$

$$q = \frac{1}{\sqrt{2}}[(\sigma_1 - \sigma_2)^2 + (\sigma_2 - \sigma_3)^2 + (\sigma_3 - \sigma_1)^2]^{1/2} \tag{20}$$

$$b = \frac{(\sigma_2 - \sigma_3)}{(\sigma_1 - \sigma_3)} \tag{21}$$

where *p'*,*q* and *b* are the mean effective stress, deviator stress and the *b-value* respectively.

6.3.3Testing Program

Three series of tests were performed using the plane strain apparatus. The first series consisted of samples C$K_0$1, C$K_0$2, and C$K_0$3. This series was used to verify that the control program for K_0 consolidation worked as desired. Once the control program was found satisfactory, a series of drained and undrained tests were performed in order to compare with previous work performed with this plane strain apparatus. Series 2 consisted of three drained plane strain tests (PSCK_0D01, PSCK_0D02, and PSCK_0D03) and Series 3 consisted of three undrained plane strain tests (PSCK_0U04, PSCK_0U05, and PSCK_0U06). A summary of the undrained plane strain tests is given in Table 6-3.

Table 6-3. Summary of plane strain tests

Sample Number	e_o	e_c	Consolidation Pressure (kPa)	Stress State after consolidation		K_0
				pc'	qc	
C$K_0$01	0.757	0.739	106	Samples not sheared		0.475
C$K_0$02	0.750	0.736	101			0.480
C$K_0$03	0.756	0.743	100			0.525
PSCK_0D01	0.798	0.783	105	67.8	55.8	0.439
PSCK_0D02	0.776	0.749	207	138.8	101.9	0.489
PSCK_0D03	0.791	0.763	306	203.9	153.1	0.493
PSCK_0U04	0.817	0.790	105	74.1	47.0	0.538
PSCK_0U05	0.787	0.763	220	140.8	104.4	0.505
PSCK_0U06	0.800	0.769	325	209.6	173.6	0.467

6.4Results & Discussion

6.4.1Results of the K_0 Consolidation Control Program

A series of three loose sand samples (C$K_0$01-C$K_0$03) were prepared in order to test the control program written for the K_0 consolidation stage of the plane strain test. The testing parameters of the samples can be seen in Table 6-3. Figure 6-10(a) depicts the axial strain versus the log of the vertical effective stress during consolidation. Samples C$K_0$01, C$K_0$02, and C$K_0$03 were consolidated to a vertical effective stress of 106 kPa, 101 kPa, and 100 kPa. Figure 6-10(b) shows the axial strain versus volumetric strain during consolidation. During K_0 consolidation, the ratio of volumetric strain to axial strain was kept at a constant value of 1 ($\frac{d\varepsilon_v}{d\varepsilon_1} = 1$) so that no lateral strain developed in the sample. The coefficient of linearity between the axial and the volumetric deformation was nearly 1 throughout the entirety of each test. This ensures that there was little lateral deformation during the consolidation of the sample. Figure 6-10(c) shows the coefficient of lateral earth pressure (K_0) during consolidation. The coefficient of lateral earth pressure for samples C$K_0$01, C$K_0$02, and C$K_0$03 was found to be 0.475, 0.480, and 0.525. It was observed that

the coefficient of lateral earth pressure became linear around an axial strain of 0.2% for all three samples. Figure 6-10(d) depicts the effective stress paths for the three samples during consolidation.

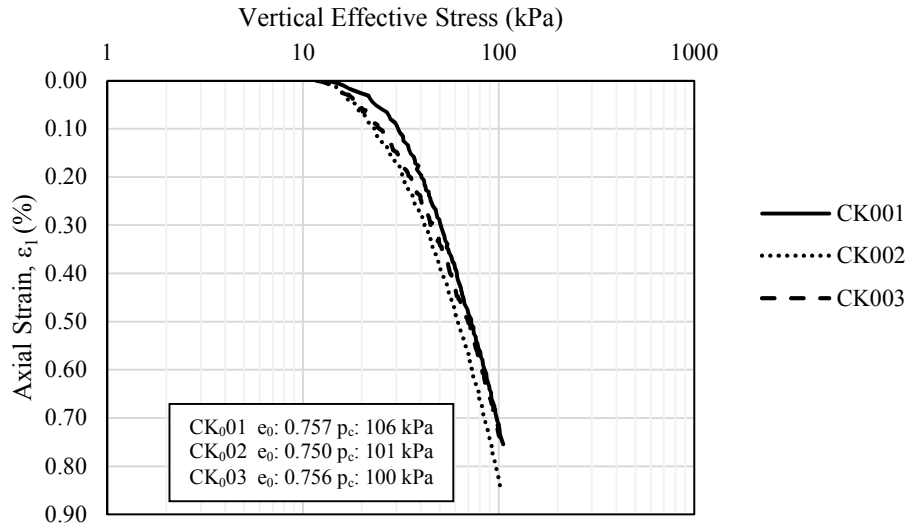

Figure 6-10(a).Compression curve

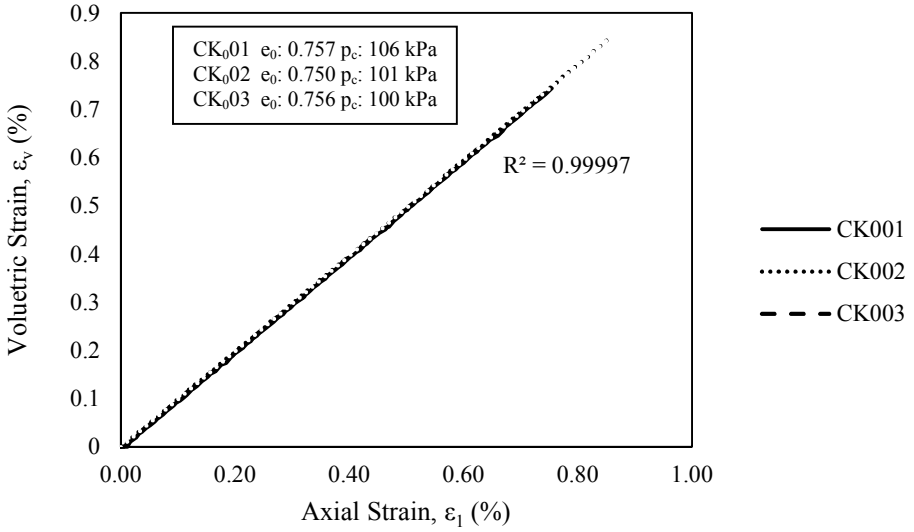

Figure 6-10(b).Axial strain versus volumetric strain during consolidation

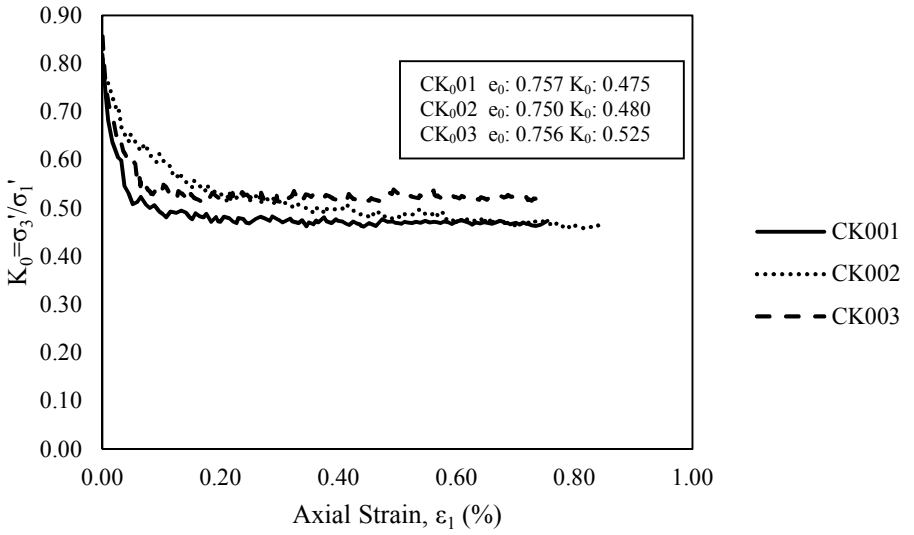

Figure 6-10(c).*K₀* versus axial strain

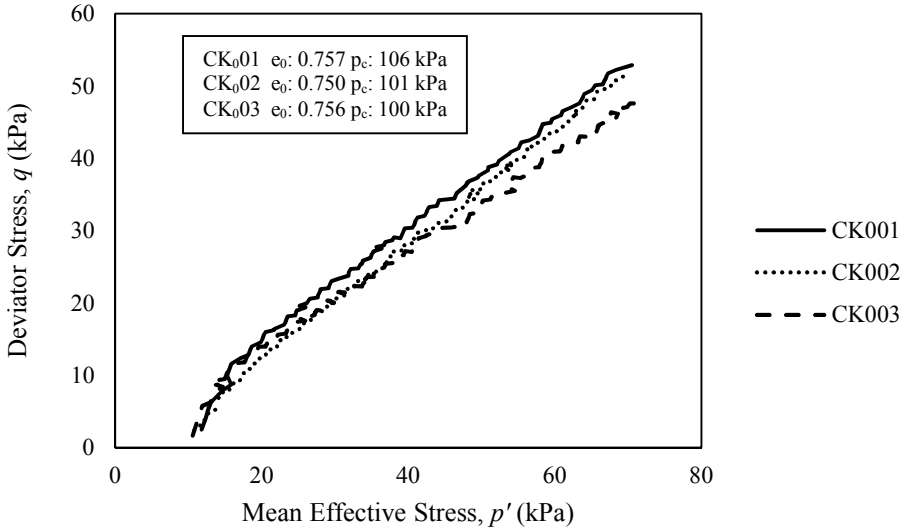

Figure 6-10(d). Effective stress path during consolidation

Figure 6-10. Results of control program (a) compression curve; (b) axial and volumetric strain; (c) K_0 versus axial strain curves; and (d) effective stress path during consolidation

It was mentioned previously that the plane strain apparatus used in this study allows for the measurement of lateral pressure (σ_2). Due to this, during the shearing stage of all plane strain tests $\sigma_2' \neq \sigma_3'$. However, during K_0 consolidation under plane strain conditions,

it was observed that σ_2' was nearly identical with that of σ_3'. Since σ_2' and σ_3'are nearly the same throughout the consolidation portion of the test, either value can be used to calculate the coefficient of lateral earth pressure K_0.

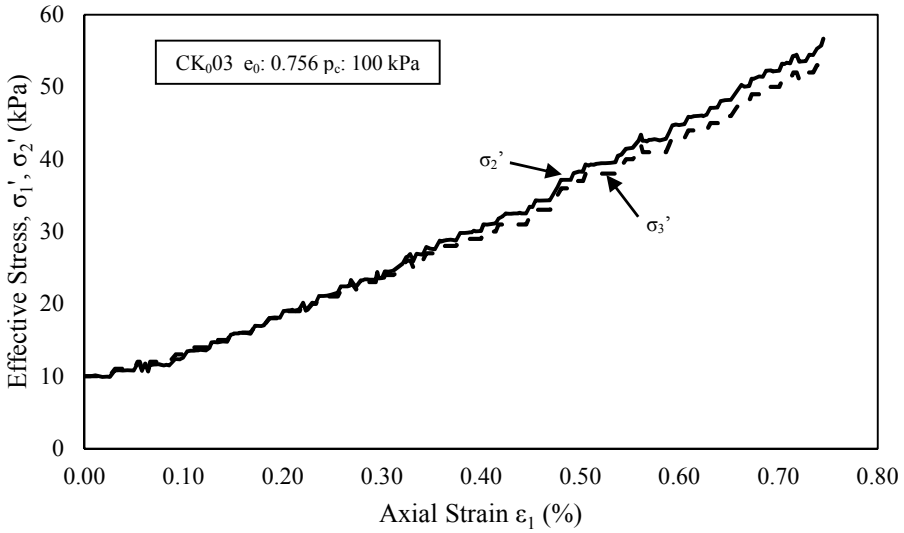

Figure 6-11. Lateral Stress response under K_0 consolidation under plane strain condition

6.4.2Drained Behavior of Loose Sand

The results of the CK_0D test on loose sand is presented below in Figure 6-12. The effective stress paths are shown in Figure 6-12(a). The gradient of the failure line was found to be around 1.02. The drained tests show an increasing trend from the point at the end of consolidation up to the failure line. Once reaching the failure line, both the deviator stress and mean effective stress increases along the failure line. The stress-strain curves are shown in Figure 6-12(b). The deviator stress q approached a constant value near the end of the test. It was observed that the maximum deviator stress increased with increasing confining pressure. Figure 6-12(c) indicates that the volumetric strain also approached a

constant value at the end of the test. This indicates that the failure line in figure 6-12(a) is also the critical state line (CSL).

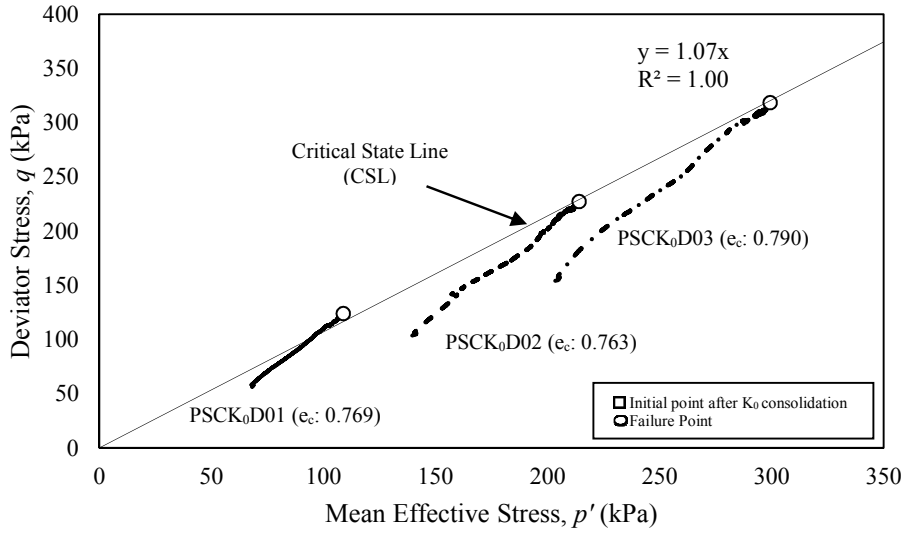

Figure 6-12(a). Effective stress paths

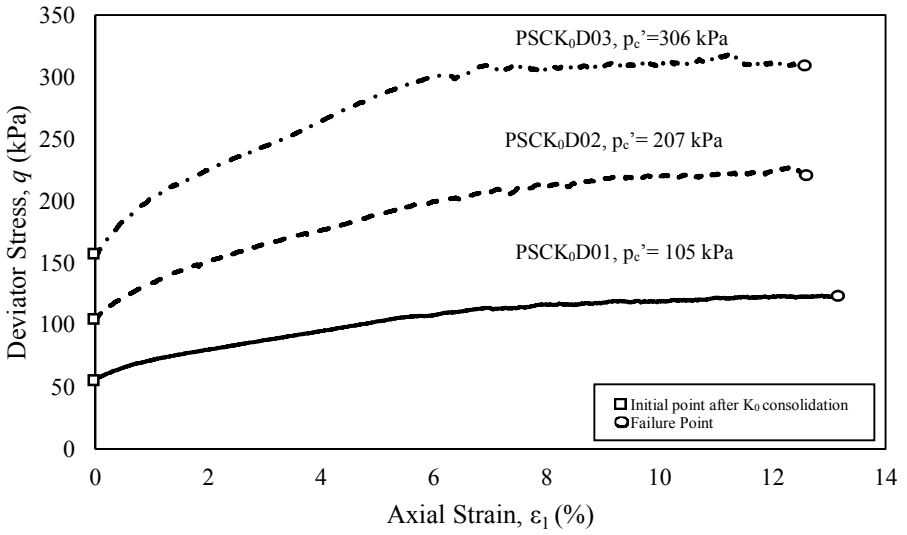

Figure 6-12(b). Shear stress versus axial strain

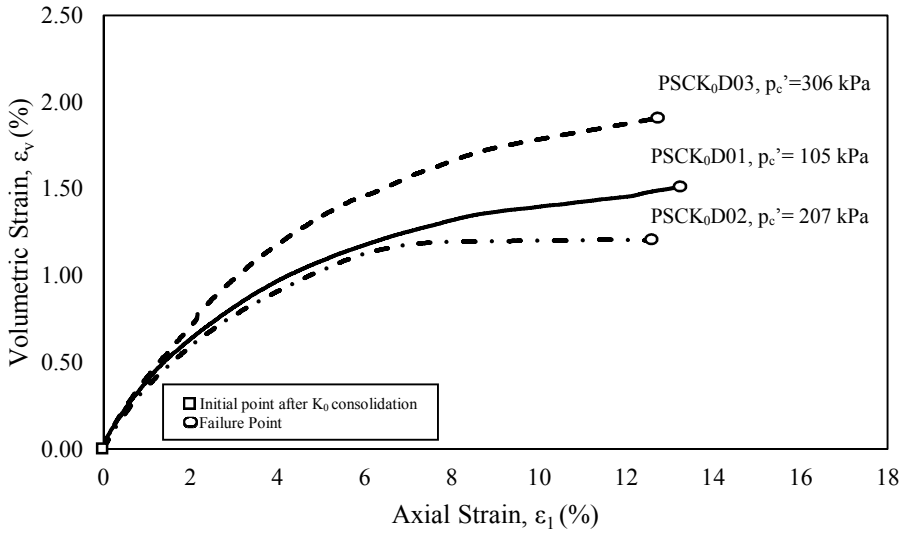

Figure 6-12(c). Axial strain versus volumetric strain

Figure 6-12. Drained behavior of loose sand: (a) effective stress paths; (b) stress-strain behavior; (c) volume change behavior

6.4.3Undrained Behavior of Loose Sand

The results of three K_0 consolidated undrained tests PSCK_0U04, PSCK_0U05, and PSCK_0U06 are presented in Figure 6-13. The void ratio after K_0 consolidation, e_c, of the three undrained specimens were 0.790, 0.763, and 0.769. Samples PSCK_0U04, PSCK_0U05, and PSCK_0U06 were K_0 consolidated to a vertical effective stress of 105, 210, and 325 kPa.

The effective stress paths as determined from the three undrained tests are presented in Figure 6-13(a). The critical state line (CSL) which was determined from the failure point of the three undrained tests is also given in Figure 6-13(a). It can be seen that the effective stress paths of the undrained tests approach the CSL as with the exception of PSCK_0U05 which reaches the CSL at a slightly higher point than the PSCK_0U04 and PSCK_0U06. The slope of the CSL was determined by fitting a linear trend line to the failure points of the three undrained tests. The slope of the failure line was found to be 0.98. The stress versus

strain curves from the three undrained tests are presented in Figure 6-13(b). All three samples exhibit strain softening behavior. For all three tests the deviator stress became constant at an axial strain of between 4% and 6%. It should be noted that there was no observed "peak" shear stress. This is likely due to the sampling frequency of the data logger. The interval between data readings in all of the tests was 5 seconds. A shorter sampling frequency should allow a visible peak to form on the stress strain curve shown in Figure 6-13(b). The excess pore water pressure versus axial strain is shown in Figure 6-13(c). All three undrained samples exhibited an increase in pore water pressure typical of the contractive behavior of loose sands. The excess pore water pressure became constant at an axial strain of between 4% and 6% similar to the stress versus strain curves signifying that the steady state had been reached.

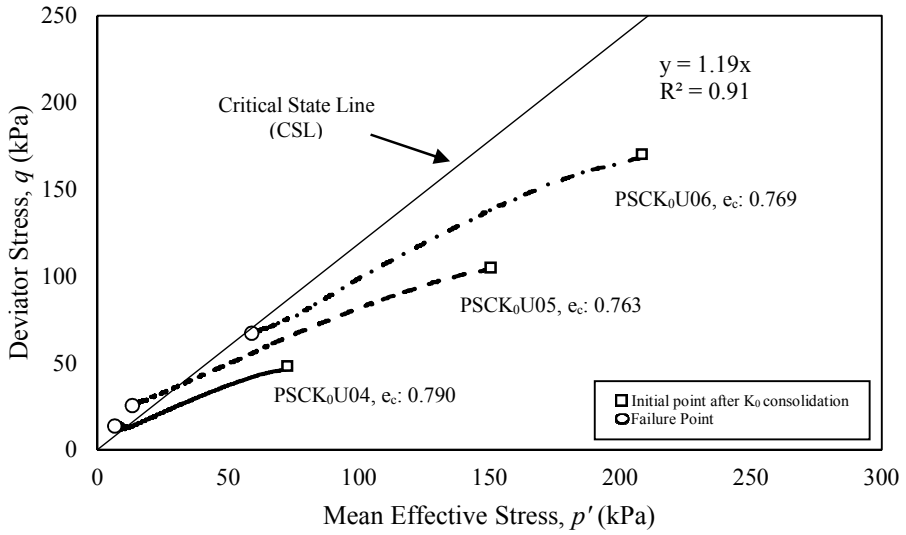

Figure 6-13(a). Effective stress path

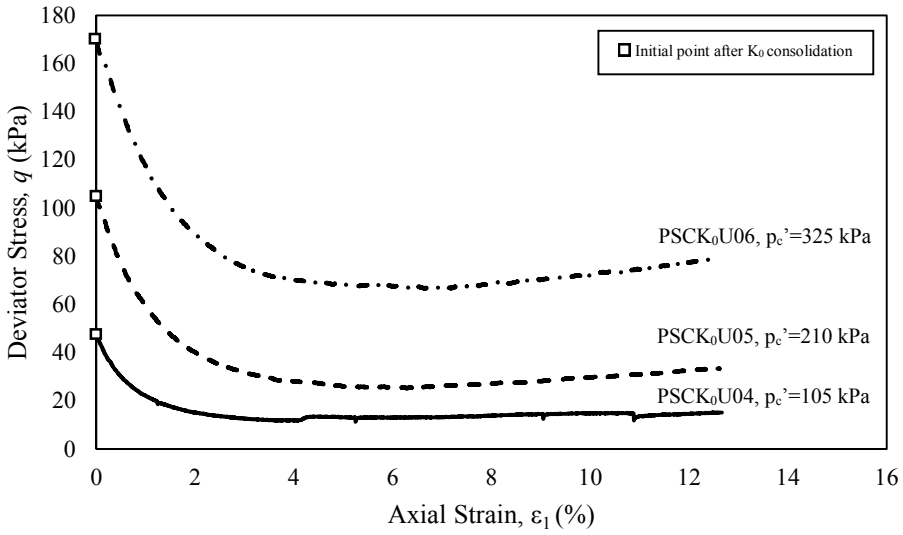

Figure 6-13(b).Stress strain curves

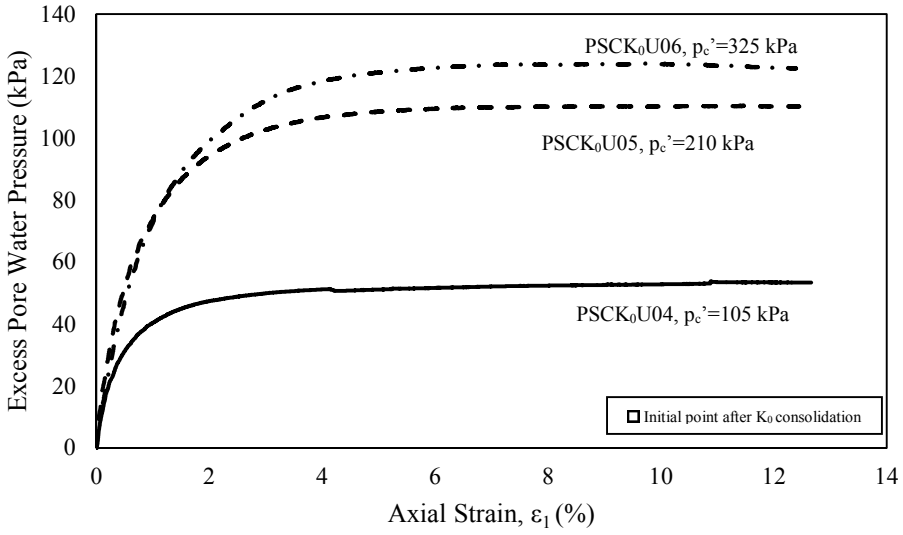

Figure 6-13(c).Excess pore water pressure versus axial strain

Figure 6-13. Undrained behavior of loose sand: (a) effective stress paths; (b) stress-strain curves; (c) excess pore water pressure versus axial strain

6.4.4Comparison of Plane Strain Tests and Triaxial Tests

A comparison between the undrained and drained plane strain tests are shown in Figure 6-14. As can be seen from the figure the CSL for the undrained tests shows a failure

line that is higher than the CSL found under drained conditions. The slope of the CSL line was found to be 1.19 for the undrained tests and 1.07 for the drained tests. While the slopes of the CSL line should be similar for both undrained and drained, the high value of the deviator stress at the failure points of the undrained tests is the cause for the higher CSL slope found under undrained conditions. This is likely due to the non-linear failure envelope. Should samples with higher failure states be performed the slope of the CSL for undrained conditions will flatten out and be closer to the value obtained under drained conditions.

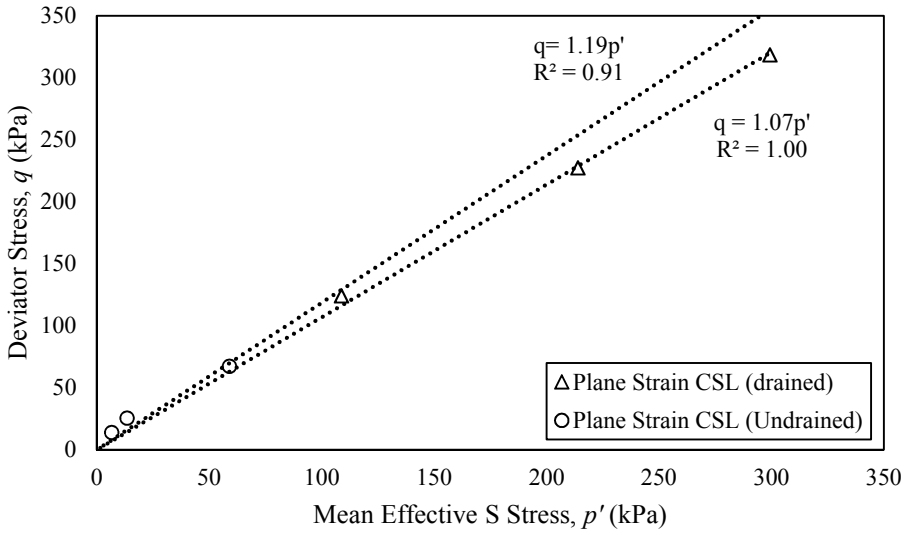

Figure 6-14. Comparison of undrained and drained plane strain tests

A comparison of the critical state lines obtained under plane strain conditions with those obtained under axisymmetric conditions is given Figure 6-15. Figure 6-15 shows that the slope of the critical state line under axisymmetric conditions is higher than that obtained under plane strain conditions. This confirms what has been presented in the literature by Wanatowski (2005) using a similar device. The slope of the CSL found under isotropic and

K_0 consolidated triaxial tests was found to be 1.20 and 1.30 while the slope of the CSL for the drained plane strain tests was found to be 1.07. The reason for these differences is the mean effective stress at failure is due to the mean effective stress (p') at failure. The value p' at failure for the K_0 triaxial tests was lower than the p' at failure under isotropic conditions. It is known that the actual failure line of soils is not linear with a higher point of failure under lower stress states. Since the mean effective stress of the K_0 was lower than the isotropic samples at failure, the slope of the CSL is higher under the K_0 conditions as compared to the isotropic tests.

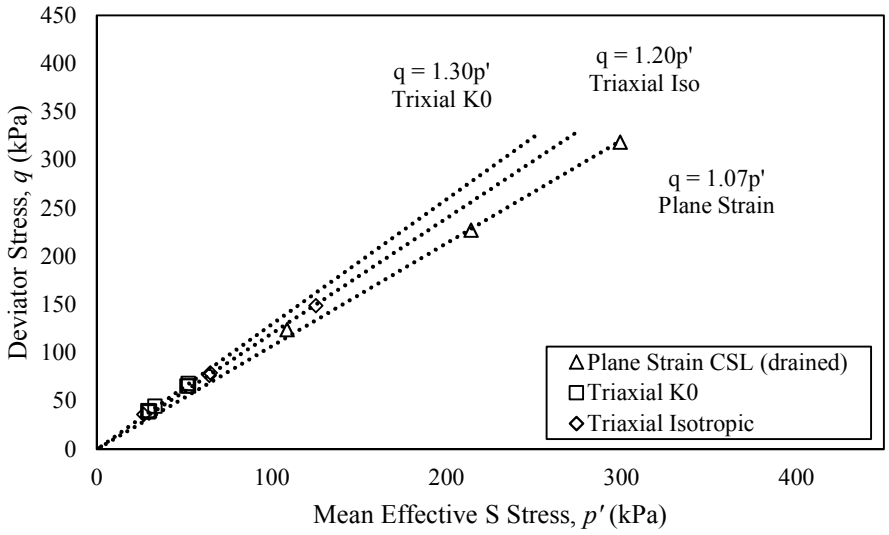

Figure 6-15. Comparison of plane strain and triaxial tests

The friction angle for the triaxial tests was calculated using the following relationship between the slope of the CSL and the friction angle.

$$\varphi' = \sin^{-1}\frac{3M}{6+M} \tag{22}$$

where φ' is the friction angle and M is slope of the critical state line. The friction angle for the plane strain tests was determined from the following equation.

$$\sin\varphi' = \frac{R-1}{R+1} \quad (23)$$

$$R = \frac{\sigma_{1f}'}{\sigma_{3f}'} \quad (24)$$

where φ' is the friction angle and R is the ratio between the major and minor principal effective stresses.

Using equation (21), the effective friction angle for the isotropic and K_0 triaxial tests was found to be 30.0^0 and 32.3^0. Using equation (22) and equation (23) the average effective friction angle for the plane strain tests was found to be slightly higher with a friction angle of 34.3^0.

6.5Conclusion

The design of an automated plane strain device has been presented in this chapter. The main feature of this plane strain apparatus is that the lateral stress (σ_2) can be measured by four submersible pressure cells throughout the entirety of the plane strain test. By measuring the lateral stress in four different locations, non-homogenous stresses and deformations can be aptly identified. Properly lubricated free-ends were used to allow for the formation of shear bands although no shear bands were observed in this study. In addition to reducing the boundary effect, the lubricated free-ends allow the shear band to develop freely.

The main objective of this chapter was to verify that the plane strain device was able to perform K_0 consolidation and undrained and drained tests on loose sand. It has been shown that the automated plane strain system allows for accurate control of K_0

consolidation and both undrained and drained shearing. It was observed, that the effective friction angle for the plane strain tests was higher than that of the triaxial tests while the slope of the CSL of the plane strain tests was lower than that of the triaxial tests. This is what has been found in the literature. In conclusion, the plane strain apparatus was proven to be reliable for the testing of granular soil under undrained and drained plane strain conditions.

CHAPTER 7.

CONCLUSIONS & RECOMMENDATIONS

7.1Conclusions

7.1.1Conclusions from Triaxial Results

The following conclusions can be made as a result of the tests performed in this study:

1. The results of the isotropically consolidated samples showed that a loose sand can go from strain softening at a fully saturated state to that of strain hardening by changing the degree of saturation through the denitrification process.
2. Under isotropic conditions, it was observed that by reducing the degree of saturation to around 89%, the peak shear stress can be increased from 25 kPa to a peak shear stress of 60 kPa.
3. However, it was observed that loose sand consolidated along the K_0 line showed very little improvement compared to the isotropically consolidated samples. Samples that were K_0 consolidated showed similar peak shear strengths as well as similar amounts of pore water pressure generation during undrained shearing regardless of the degree of saturation.
4. It was observed that the peak shear stress of the microbially treated K_0 specimens was held for a longer period of time than the fully saturated K_0 specimens. However, the magnitude was observed to be similar to the fully saturated state.

5. It was also observed that the rate of pore water pressure generation decreased for partially saturated sand as compared to the fully saturated state. However, the magnitude of the peak shear stress and the maximum pore water pressure was similar in all K_0 consolidated tests regardless of the degree of saturation.

7.1.2Conclusions from Permeability Tests

The following conclusions can be made as a result of the tests performed in this study:

1. Microbial denitrification can be used to reduce the hydraulic conductivity of sand by introducing nitrogen gas bubbles into the void spaces.
2. It was observed that the hydraulic conductivity can be reduced by 67% by decreasing the degree of saturation from around 100% to 70.9%.
3. Based upon the results of the permeability tests performed in this study, the introduction of gas bubbles in clean sand through the denitrification process does not reduce the permeability significantly enough for practical use in clean sands.

7.1.3Conclusions from Plane Strain Tests

1. It has been shown that the automated plane strain system allows for accurate control of K_0 consolidation. This was achieved by controlling the ratio of axial strain to volumetric strain. A coefficient of linearity of 0.9999 between the axial strain and the volumetric strain indicates that no lateral deformation occurred during consolidation.

2. The main feature of this plane strain apparatus is that the lateral stress (σ_2) can be measured by four submersible pressure cells throughout the plane strain test. This was used to further verify that no lateral strain occurred during K_0 consolidation as the difference between the cell pressure (σ_3) and the "out-of-plane" stress (σ_2) was very small.
3. The undrained and drained tests on loose sand verified that the control programs written for each mode of shearing resulted in the expected response of undrained and drained behavior of loose sand.
4. It was observed that the slope of the critical state line under axisymmetric conditions was higher than the slope of the critical state line under plane strain conditions. However, the friction angle under axisymmetric conditions was found to be 30.0° while the friction angle found under plane strain conditions was found to be slightly higher at 34.3°.

7.2Recommendations

The following recommendations are made as a result of this study:

1. Carry out more K_0 and/or anisotropic consolidated undrained tests to establish the influence of bio desaturation on the undrained behavior or liquefaction resistance of sand.
2. Evaluate the effect of biogas desaturation on the undrained behavior of sand under plane strain conditions by performing plane strain tests.

REFERENCES

Achal, V., Mukerjee, A., and Sudhakara Reddy, M. (2013). "Biogenic treatment improves the durability and remediates the cracks of concrete structures." *Construction and Building Materials*, 48, 1–5.

Alarcon-Guzman, A., Leonards, G. A., and Chameau, J. L. (1988). "Undrained Monotonic and Cyclic Strength of Sands." *Journal of Geotechnical Engineering*, 114(10), 1089–1109.

Alshibli, A. K., Godbold, D. L., and Hoffman, K. (2004). "The Louisiana plane strain apparatus for soil testing." *Geotech. Testing J., ASTM*, 27(4), 1–10.

Altun, S., and Goktepe, A. B. (2006). "Cyclic Stress-Strain Behavior of Partially Saturated Soils." *Unsaturated soils 2006*, 497–507.

Arthur, J. R. F., Dunstan, T., and Enstad, G. G. (1985). "Determination of the flow function by means of a cubic plane strain tester." *Int. J. Bulk Storage Silos*, 1(2), 7–10.

ASTM D2487-11. (2011). "Standard Practice for Classification of Soils for Engineering Purposes." ASTM International, West Conshohocken, PA.

ASTM D4254-14. (2014). "Standard Test Methods for Minimum Index Density and Unit Weight of Soils and Caclulation of Relative Density." ASTM International, West Conshohocken, PA.

ASTM D4253-14. (2014). "Standard Test Methods for Maximum Index Density and Unit Weight of Soils Using a Vibratory Table." ASTM International, West Conshohocken, PA.

Barden, L., Ismail, H., and Tong, P. (1969). "Plane strain deformation of granular material at low and high pressures." *Geotechnique*, 19(4), 441–452.

Been, K., and Jefferies, M. G. (1985). "A state parameter for sand." *Geotechnique*, 35(2), 99–112.

Bishop, A. W. (1955). "The use of the slip circle in the stability of slopes." *Geotechnique*, 5(1), 7–17.

Bishop, A. W. (1958). "The requirements for measuring the coefficient of earth pressure at rest." *Proc. European Conf. Earth Pressures, Brussels*, 1, 1–7.

Bishop, A. W. (1966). "Strength of soil as engineering materials (6th Rankine Lecture)." *Geotechnique*, 16(2), 89–130.

Blaszczyk, M., Galka, E., and Mycielski, R. (1985). "Denitrification of High-Concentrations of Nitrites and Nitrates in Synthetic Medium with Different Sources of Organic Carbon." *Acta Microbiologica Polonica*, 34(2), 195–205.

Bouferra, R., Benseddiq, N., and Shahrour, I. (2007). "Saturation and Preloading Effects on the Cyclic Behavior of Sand." *International Journal of Geomechanics*, 7(5), 396–401.

Campanella, R. G., and Vaid, Y. P. (1973). "Influence of stress path on the plane strain behavior of a sensitive clay." *Proc. 8th Int. Conf. Soil Mech. Found. Engng, Moscow*, 1(85-92).

Casagrande, A. (1936). "Characteristics of cohesionless soils affecting the stability of earth fills." *Contributions to Soil Mechanics: 1925-1940*, Boston Society of Civil Engineers, 257–276.

Chu, J., Ivanov, V., He, J., Naeimi, M., Li, B., and Stabnikov, V. (2011). "Development of Microbial Geotechnology in Singapore J. Chu, V. Ivanov, J. He, M. Naeimi, B. Li and V. Stabnikov." *Geo-Frontiers 2011: Advances in Geotechnical Engineering*, 4070–4078.

Chu, J., Leong, W. K., Loke, W. L., and Wanatowski, D. (2012a). "Instability of Loose Sand under Drained Conditions." *Journal of Geotechnical and Geoenvironmental Engineering*, 138(2), 207–216.

Chu, J., Stabnikov, V., and Ivanov, V. (2012b). "Microbially Induced Calcium Carbonate Precipitation on Surface or in the Bulk of Soil." *Geomicrobiology Journal*, 29, 544–549.

Chu, J., and Wanatowski, D. (2008). "Instability Conditions of Loose Sand in Plane Strain." *Journal of Geotechnical and Geoenvironmental Engineering*, 134(1), 136–142.

Chu, J., and Wanatowski, D. (2009). "Effect of Loading Mode on Strain Softening and Instability Behavior of Sand in Plane-Strain Tests." *Journal of Geotechnical and Geoenvironmental Engineering*, 135(1), 108–120.

Cornforth, D. H. (1961). "Plane strain failure characteristics of a saturated sand." University of London.

Cornforth, D. H. (1964). "Some experiments on the influence of strain conditions on the strength of sand." *Geotechnique*, 14(2), 143–167.

DeJong, J. T., Fritzges, M. B., and Nüsslein, K. (2006). "Microbially Induced Cementation to Control Sand Response to Undrained Shear." *Journal of Geotechnical and Geoenvironmental Engineering*, 132(11), 1381–1392.

DeJong, J. T., Mortensen, B. M., Martinez, B. C., and Nelson, D. C. (2010). "Bio-mediated soil improvement." *Ecological Engineering*, 36, 197–210.

Drescher, A., Vardoulakis, I. G., and Han, C. (1990). "A biaxial apparatus for testing soils." *Geotechnical Testing Journal, ASTM*, 13(3), 226–234.

Duncan, J. M., and Seed, H. B. (1966). "Strength variation along failure surfaces in clay." *Journal of Soil Mechanics & Foundations Div., ASCE*, 92(6), 81–104.

Eseller-Bayat, E. E. (2009). "Seismic response and prevention of liquefaction failure of sands partially saturated through introduction of gas bubbles." *Civil and Environmental Engineering*, PhD, 262.

Finno, R. J., Harris, W. W., Mooney, M. A., and Viggiani, G. (1997). "Shear bands in plane strain compression of loose sand." *Geotechnique*, 47(1), 149–165.

Finno, R. J., Harris, W. W., and Viggiani, G. (1996). "Strain localization and undrained steady state of sand." *J. Geotech. Engng, ASCE*, 122(6), 462–473.

Fredlund, D. G., and Rahardjo, H. (1993). "Flow Laws." *Soil Mechanics for Unsaturated Soils*, John Wiley & Sons, New York, 110–113.

Glass, C., and Silverstein, J. (1998). "Denitrification Kinetics of High Nitrate Concentration Water: pH Effect on Inhibition and Nitrite Accumulation." *Water Research*, 32(3), 831–839.

Green, G. E. (1971). "Strength and deformation of sand measured in an independent stress control cell." *Proceedings Roscoe Memorial Symposium: "Stress-strain behavior of soils,"* Cambridge University, 285–323.

Green, G. E., and Reades, A. W. (1975). "Boundary conditions, anisotropy and sample shape effects on the stress-strain behavior of sand in triaxial compression and plane strain." *Geotechnique*, 25(2), 333–356.

Grozic, J. L., Robertson, P. K., and Morgenstern, N. R. (1999). "The behavior of loose gassy sand." *Canadian Geotechnical Journal*, 36, 482–492.

Hambly, E. C. (1969). "A new true triaxial apparatus." *Geotechnique*, 19(2), 307–309.

Hambly, E. C. (1972). "Plane strain behavior of remoulded normally consolidated kaolin." *Geotechnique*, 22(2), 301–317.

Hambly, E. C., and Roscoe, K. H. (1969). "Observations and predictions of stresses and strains during plane-strain of 'wet' clays." *Proc. 7th Int. Conf. Soil Mech. Found. Engng, Mexico*, 1(173-181).

Han, C., and Vardoulakis, I. G. (1991). "Plane-strain compression experiments on water-saturated fine-grained sand." *Geotechnique*, 41(1), 49–78.

Harkes, M. P., van Paassen, L. a., Booster, J. L., Whiffin, V. S., and van Loosdrecht, M. C. M. (2010). "Fixation and distribution of bacterial activity in sand to induce carbonate precipitation for ground reinforcement." *Ecological Engineering*, 36, 112–117.

Harris, W. W., Viggiani, G., Mooney, M. A., and Finno, R. J. (1995). "Use of stereophotogrammetry to analyze the development of shear bands in sand." *Geotechnical Testing Journal*, 18(4), 405–420.

He, J. (2013). "Mitigation of Liquefaction of Sand Using Microbial Methods." Nanyang Technological University.

He, J., and Chu, J. (2013). "Undrained Responses of Microbially Desaturated Sand under Monotonic Loading." *Journal of Geotechnical and Geoenvironmental Engineering*, 140(5).

He, J., Chu, J., and Liu, H. (2014). "Undrained shear strength of desaturated loose sand under monotonic shearing." *Soils and Foundations*, Elsevier, 1–7.

John, P. (1977). "Aerobic and anaerobic bacterial respiration monitored by electrodes." *Journal of General Microbiology*, (98), 231–238.

Knowles, R. (1982). "Denitrification." *Microbiological Reviews*, 46(1), 43–70.

Ko, H. Y., and Davidson, L. W. (1973). "Bearing capacity of footings in plane strain." *J. Soil Mech. and Found. Div., ASCE*, 99(1), 1–23.

Lambe, T. W., and Whitman, R. V. (1979). *Soil Mechanics*. New York: Wiley.

Lee, J.-S., and Santamarina, J. C. (2007). "Seismic Monitoring short-duration events: liquefaction in 1g models." *Canadian Geotechnical Journal*, 44, 659–672.

Lee, K. L. (1970). "Comparison of plane strain and triaxial tests on sand." *Journal of Soil Mechanics & Foundations Div*, 96(3), 901–923.

Leussink, H., and Wittke, W. (1964). "Difference in triaxial and plane strain shear strength." *Laboratory shear testing of soils, ASTM STP*, 361, 77–89.

Little, A. L., and Price, V. E. (1958). "The use of an electric computer for slope stability analysis." *Geotechnique*, 8(3), 113–120.

Marachi, N. D., Duncan, J. M., Chan, C. K., and Seed, H. B. (1981). "Plane-strain testing of sand." *Laboratory shear strength of soil, ASTM STP*, 740, 294–302.

Oda, M., Koshikawa, I., and Higuchi, T. (1978). "Experimental study of anisotropic shear strength of sand by plane strain test." *Soils and Foundations*, 18(1), 25–38.

Okamura, M., Ishihara, M., and Oshita, T. (2003). “Liquefaction Resistance of Sand Deposit Improved with Sand Compaction Piles.” *Japanese Geotechnical Society*, 43(5).

Okamura, M., and Soga, Y. (2006). “Effects of Pore Fluid Compressbility on Liquefaction Resistance of Partially Saturated Sand.” *Soils and Foundations*, 46(5), 695–700.

Okamura, M., Takebayashi, M., Nishida, K., Fujii, N., Jinguji, M., Imasato, T., Yasuhara, H., and Nakagawa, E. (2011). “In-Situ Desaturation Test by Air Injection and Its Evaluation through Field Monitoring and Multiphase Flow Simulation.” *Journal of Geotechnical and Geoenvironmental Engineering*, 137(7), 643–652.

Okamura, M., and Teraoka, T. (2006). “Shaking Table Tests to Invesitage Soil Desaturation as a Liquefaction Countermeasure.” *Seismic Performance and Simulation of Pile Foundations in Liquified and Laterally Spreading Ground*, 282–293.

Van Paassen, L. a., Daza, C. M., Staal, M., Sorokin, D. Y., van der Zon, W., and van Loosdrecht, M. C. M. (2010). “Potential soil reinforcement by biological denitrification.” *Ecological Engineering*, 36, 168–175.

Van Passen, L. A., Daza, C. M., Staal, M., Sorokin, D. Y., van der Zon, W., and van Loosdrecht, M. C. . (2010). “Potential Soil Reinforcement by Biological Denitrification.” *Ecological Engineering*, 36(2), 168–175.

Pietruszczak, S., Pande, G. N., and Oulapour, M. (2003). “A hypothesis for mitigation of risk of liquefaction.” *Géotechnique*, 53(9), 833–838.

Poulos, S. J. (1981). “The Steady State of Deformation.” *J. Geotech. Engng, ASCE*, 107(5), 553–562.

Rad, N., Vianna, A., and Berre, T. (1994). “Gas in Soils. II: Effect of Gas on Undraiend Static and Cyclic Strength of Sand.” *Journal of Geotechnical Engineering*, 120(4), 716–736.

Rebata-Landa, V., and Santamarina, J. (2012). “Mechanical effects of biogenic nitrogen gas bubbles in soils.” *Journal of Geotechnical and …*, (2), 128–137.

Rowe, P. W. (1969). “The relation between the shear strength of sand in triaxial compression, plane strain, and direct shear.” *Geotechnique*, 19(1), 75–86.

Rowe, P. W., and Barden, L. (1964). “Importance of Free Ends in Triaxial Testing.” *Journal of Soil Mechanics & Foundations Div*, 90(1), 1–27.

Saleh-Lakha, S., Shannon, K. E., Henderson, S. L., Goyer, C., Trevors, J. T., Zebarth, B. J., and Burton, D. L. (2009). “Effect of pH and temperature on denitrification gene

expression and activity in Pseudomonas mandelii." *Applied and Environmental Microbiology*, 75(12), 3903–3911.

Schofield, A. N., and Wroth, C. P. (1968). *Critical State Soil Mechanics*. McGraw-Hill, London.

Sherif, M. A., Tsuchiya, C., and Ishibashi, I. (1977). "Saturation Effect on Initial Soil Liquefaction." *Journal of Geotechnical Engineering*, 103(8), 914–917.

Skempton, A. W. (1986). "Standard penetration test procedures and the effects in sands of overburden pressure, relative density, particle size, ageing and overconsolidation." *Geotechnique*, 34(3), 425–447.

Stabnikov, V., Naeimi, M., Ivanov, V., and Chu, J. (2011). "Formation of water-impermeable crust on sand surface using biocement." *Cement and Concrete Research*, 41, 1143–1149.

Stanford, G., Vander Pol, R. A., and Dzienia, S. (1975). "Denitrification rates in relation to total and extractable soil carbon." *Soil Science Society of America Proceedings*, (39), 284–289.

Tamura, S., Tokimatsu, K., Abe, A., and Sato, M. (2002). "Effects of Air Bubbles on B-Value and P-wave velocity of a partially saturated sand." *Soils and Foundations*, 42(1), 121–129.

Tatsuoka, F., Sakamoto, M., Kawamura, T., and Fukushima, S. (1986). "Strength and deformation characteristics of sand in plane strain compression at extremely low pressures." *Soils and Foundations*, 26(1), 65–84.

Tatsuoka, F., Sato, T., Park, C., Kim, Y. S., Mukabi, J. N., and Kohata, Y. (1994). "Measuring of elastic properties of geomaterials in laboratory compression tests." *Geotech. Testing J., ASTM*, 17(1), 80–94.

Topolnicki, M., Gudehus, G., and Mazurkiewicz, B. K. (1990). "Observed stress-strain behavior of remoulded saturated clay under plane-strain conditions." *Geotechnique*, 42(2), 155–187.

Trautwein. (2004). "GeoTAC Truepath Instruction Manual-Version 5.3.5." Trautwein Soil Testing Equipment Company.

Tsukamoto, Y., Ishihara, K., Nakazawa, H., Kamada, K., and Huang, Y. (2002). "Resistance of Partly Saturated Sand to Liquefaction with Reference to Longitudinal and Shear Wave Velocities." *Soils and Foundations*, 42(6), 93–104.

Vermeer, P. A. (1990). "The Orientation of shear bands in biaxial tests." *Geotechnique*, 40(2), 223–236.

Wanatowski, D. (2005). “Strain Softening and Instability of Sand under Plane-Strain Conditions.” Nanyang Technological University.

Wanatowski, D., and Chu, J. (2007a). “Static liquefaction of sand in plane strain.” *Canadian Geotechnical Journal*, 44(3), 299–313.

Wanatowski, D., and Chu, J. (2007b). “A New Plane-Strain Apparatus and Plane-Strain Tests on Sand.” *Proc. the 16th Southeast Asian Geotechnical Conference*, Subang Jaya, Malaysia, 393–398.

Wanatowski, D., and Chu, J. (2008). “Effect of Specimen Preparation Method on the Stress-Strain Behavior of Sand in Plane-Strain Compression Tests.” *Geotechnical Testing Journal, ASTM*, 31(4), 308–320.

Wanatowski, D., Chu, J., and Loke, W. L. (2010). “Drained instability of sand in plane strain.” *Canadian Geotechnical Journal*, 47(4), 400–412.

Whiffin, V. S., van Paassen, L. a., and Harkes, M. P. (2007). “Microbial Carbonate Precipitation as a Soil Improvement Technique.” *Geomicrobiology Journal*, 24(5), 417–423.

Wilhelm, E., Battino, R., and Wilcock, R. J. (1977). “Low-Pressure Solubility of Gases in Liquid Water.” *Chemical Reviews*, 77(2), 219–262.

Xia, H., and Hu, T. (1991). “Effects of Saturation and Back Pressure on Sand Liquefaction.” *Journal of Geotechnical Engineering*, 117(9), 1347–1362.

Yang, J. (2002). “Non-uniqueness of flow liquefaction line for loose sand.” *Geotechnique*, 52(10), 757–760.

Yasin, S. J. M., Umetsu, K., Tatsuoka, F., Arthur, J. R. F., and Dunstan, T. (1999). “Plane-strain strength and deformation of sands by batch variations and different apparatus types.” *Geotechnical Testing Journal, ASTM*, 22(1), 80–100.

Yegian, M. K., Eseller, E., and Alshawabkeh, A. (2006). “Preperation and Cyclic Testing of Partially Saturated Sands.” *Unsaturated Soils 2006*, 508–518.

Yegian, M. K., Eseller-Bayat, E., Alshawabkeh, a., and Ali, S. (2007). “Induced-Partial Saturation for Liquefaction Mitigation: Experimental Investigation.” *Journal of Geotechnical and Geoenvironmental Engineering*, 133(4), 372–380.

Yoshimi, Y., Tanaka, K., and Tokimatsu, K. (1989). “Liquefaction Resistance of a Partially Saturated Sand.” *Soils and Foundations*, 29(3), 157–162.